HHS Public Access

Author manuscript

Glia. Author manuscript; available in PMC 2021 October 05.

Published in final edited form as:

Glia. 2021 January ; 69(1): 91–108. doi:10.1002/glia.23886.

α_V integrins in Schwann cells promote attachment to axons, but are dispensable in vivo

Kathleen K. Catignas[1,2], **Luciana R. Frick**[1,3], **Marta Pellegatta**[1,4], **Edward Hurley**[1,3], **Zachary Kolb**[2], **Kathryn Addabbo**[2], **Joseph H. McCarty**[5], **Richard O. Hynes**[6], **Arjan van der Flier**[6,7], **Yannick Poitelon**[1,2,8], **Lawrence Wrabetz**[1,2,3], **Maria Laura Feltri**[1,2,3]

[1]Hunter James Kelly Research Institute, University at Buffalo, Buffalo, New York

[2]Department of Biochemistry, University at Buffalo, Buffalo, New York

[3]Department of Neurology, Jacobs School of Medicine and Biomedical Sciences, University at Buffalo, Buffalo, New York

[4]IRCCS San Raffaele Scientific Institute and Vita Salute San Raffaele University, Milan, Italy

[5]Department of Neurosurgery, The University of Texas M.D. Anderson Cancer Center, Houston, Texas

[6]Howard Hughes Medical Institute, Massachusetts Institute of Technology, Boston, Massachusetts

[7]Sanofi, Boston, Massachusetts

[8]Department of Neuroscience and Experimental Therapeutics, Albany Medical College, Albany, New York

Abstract

In the developing peripheral nervous system, Schwann cells (SCs) extend their processes to contact, sort, and myelinate axons. The mechanisms that contribute to the interaction between SCs and axons are just beginning to be elucidated. Using a SC-neuron coculture system, we demonstrate that Arg-Gly-Asp (RGD) peptides that inhibit α_V-containing integrins delay the extension of SCs elongating on axons. α_V integrins in SC localize to sites of contact with axons and are expressed early in development during radial sorting and myelination. Short interfering RNA-mediated knockdown of the α_V integrin subunit also delays SC extension along axons in vitro, suggesting that α_V-containing integrins participate in axo-glial interactions. However, mice

Correspondence Maria Laura Feltri, Hunter James Kelly Research Institute, University at Buffalo, Buffalo, NY 14203. mlfeltri@buffalo.edu.

AUTHOR CONTRIBUTIONS

Kathleen K. Catignas, Marta Pellegatta, Luciana R. Frick, and Maria Laura Feltri designed research and interpreted data. Kathleen K. Catignas, Marta Pellegatta, and Luciana R. Frick performed experiments and data analysis with assistance from Edward Hurley, Zachary Kolb, Kathryn Addabbo, and Lawrence Wrabetz. Luciana R. Frick, Joseph H. McCarty, Richard O. Hynes, and Arjan van der Flier provided reagents. Kathleen K. Catignas, Luciana R. Frick, and Maria Laura Feltri wrote the manuscript. Maria Laura Feltri, Yannick Poitelon, Luciana R. Frick, and Lawrence Wrabetz critically reviewed the manuscript.

CONFLICT OF INTEREST

The authors declare no conflict of interest.

SUPPORTING INFORMATION

Additional supporting information may be found online in the Supporting Information section at the end of this article.

lacking the α_V subunit in SCs, alone or in combination with the potentially compensating α_5 subunit, or the α_V partners β_3 or β_8, myelinate normally during development and remyelinate normally after nerve crush, indicating that overlapping or compensatory mechanisms may hide the in vivo role of RGD-binding integrins.

Keywords

axo-glial interactions; integrin; lamellipodia; process extension; RGD; Schwann cell

1 | INTRODUCTION

Successful myelination in the peripheral nervous system (PNS) depends on the ability of Schwann cell (SC) glia to engage in cell-to-cell contact with neurons. This contact is important because some of the molecular cues that instruct immature SCs to differentiate into promyelinating SCs derive from axons, and SCs gain access to these cues by direct axon contact. Though several ligand-receptor pairs at the axo-glial interface have been identified (reviewed in Feltri, Poitelon, & Previtali, 2016; Monk, Feltri, & Taveggia, 2015), the molecular composition of this junction is far from complete.

Initially, precursor SCs receive survival and mitogenic signals from axons as they contact and migrate along them at the start of development (Jessen & Mirsky, 2005). The interaction with groups of axons then triggers immature SCs to deposit and organize basal lamina components such as laminins onto their *ab*-axonal surface (away from the axon). This basal lamina then becomes necessary to initiate radial sorting, a key premyelination step in the PNS (Feltri & Wrabetz, 2005). During radial sorting, immature SCs extend lamellipodia-like processes toward bundled axons to sort and separate larger axons destined for myelination from smaller axons destined for ensheathment by nonmyelinating Remak SCs (reviewed in Feltri et al., 2016). Finally, as a promyelinating SC attains 1:1 relationship with an axon, it extends its processes concentrically around as well as laterally along the axon to elaborate myelin (reviewed in Salzer, 2015). Fundamentally, SC development and the myelination of axons are contact-mediated phenomena.

The failure of SCs to generate the lamellipodia-like processes necessary to engage axons underlie many radial sorting and myelination defects in mice (Feltri et al., 2016). SC-specific deletion of small RhoGTPases and other cytoskeletal regulators, for instance, leads to myelination abnormalities (Benninger et al., 2007; Elbaz et al., 2016; Jin et al., 2011; Montani et al., 2014; Nodari et al., 2007; Novak et al., 2011). Also, ablating SC laminins or their cognate receptors impairs process extension; this impedes axon-SC interactions and results in profound myelination defects (Feltri et al., 2002; Yu, 2005; Yu, Chen, North, & Strickland, 2009). Many laminin receptors are integrins, Type-1 transmembrane molecules composed of α/β heterodimers that mediate cell–cell or cell–extracellular matrix (ECM) adhesion (Hynes, 1987). They link intracellular cytoskeletal components with extracellular components and govern numerous morphogenetic signaling pathways (Hynes, 2002b). We showed previously that conditionally deleting β_1-containing integrins in SCs (β_1 cKO) produces severe radial sorting defects in vivo (Feltri et al., 2002), yet deleting $\alpha_3\beta_1$, $\alpha_6\beta_1$,

and $\alpha_7\beta_1$ (three major laminin-binding integrins expressed by SCs) in single or double combinations only mildly affects radial sorting (Pellegatta et al., 2013; Previtali et al., 2003). These suggested that perhaps the inactivation of β_1 heterodimers that do not primarily bind laminins contributed to the severity of the β_1 cKO phenotype. Furthermore, β_1 heterodimers, which become strictly localized to the *ab*-axonal SC surface as myelination progresses (Feltri et al., 2002; Pellegatta et al., 2013), were also localized on SC processes *ad*-axonally (juxtaposed to the axon) while radial sorting was being performed (Berti et al., 2011). This suggested some β_1 heterodimers might function at the axo-glial interface independently of laminins.

These investigations made us focus on the largely uncharacterized roles of integrins that may bind other ligands besides laminins and led us to search for new SC molecules at the axo-glial junction (Poitelon et al., 2015). Ligands that bear an accessible RGD (Arg-Gly-Asp) or RGD-related tripeptide motif, which are quite prevalent, are recognized by some β_1-containing integrins as well as by all members of the second largest subfamily of integrins, the α_V-containing integrins (Supplemental Information Figure S1a), which are expressed by cultured SCs (Aumailley, Gerl, Sonnenberg, Deutzmann, & Timpl, 1990; Chernousov & Carey, 2003; Humphries, 2006; Milner, Wilby, et al., 1997). RGD-binding integrins like those containing α_V were long thought to be important for developing SCs and oligodendrocytes, the myelinating glia of the central nervous system (CNS). For instance, RGD peptides (decoys that block RGD receptors) hamper SC migration in vitro, suggesting RGD-binding integrins may participate in SC migration early in development (Milner, Wilby, et al., 1997). Moreover, oligodendrocyte myelination seems RGD dependent, as adding RGD peptides inhibits myelin synthesis in vitro (Cardwell & Rome, 1988). Indeed, several α_V heterodimers are postulated to participate in oligodendrocyte development (Blaschuk, Frost, & Ffrench-Constant, 2000; Milner, Frost, et al., 1997; Milner, Edwards, Streuli, & Ffrench-Constant, 1996; Milner & Ffrench-Constant, 1994; Shaw, Milner, Compston, & Ffrench-Constant, 1996). In vivo ablation of the integrin α_V subunit in the CNS and PNS using Nestin-Cre results in axonal degeneration in the CNS (McCarty et al., 2005; Mobley, Tchaicha, Shin, Hossain, & McCarty, 2009; Zimmerman et al., 1994). Interestingly, these mutant mice also develop limp paresis, which could be due to axonal Nestin-Cre expression, but it is also characteristic of impaired PNS myelination (Michelson, Russell, & Harman, 1955).

While RGD-binding integrins canonically bind ECM molecules like fibronectin (FN), vitronectin, fibrin, and the TGFβ complex, to name a few, reports from other systems show that α_V-containing integrins also bind cell surface molecules like Neuregulin-1 (NRG1) and L1 cell adhesion molecule, which are important axon-derived molecules in the PNS (Haney et al., 1999; Ieguchi et al., 2010; Itoh et al., 2005; Montgomery et al., 1996; Taveggia et al., 2005). In the CNS, $\alpha_V\beta_3$ on glial astrocytes binds axon-derived Thy1 to promote formation of astrocytic focal adhesions necessary for neuron-astrocyte communication (Leyton et al., 2001). Furthermore, axonal molecule ADAM22, which belongs to a family that binds RGD-binding integrins, is speculated to bind SC integrins in order to properly function in PNS myelination (Ozkaynak et al., 2010; Seals & Courtneidge, 2003). All together, we hypothesized that RGD-binding integrins could play a role in the PNS myelination process.

Here, we analyzed the role of RGD-binding integrins, particularly α_V-containing integrins, during SC development. Using an established in vitro coculture system that recapitulates axon-SC interactions in vivo, we demonstrate that α_V-containing integrins contribute to process extension of SCs. However, SC-specific ablation of α_V integrin in vivo has no detectable consequences.

2 | MATERIALS AND METHODS

2.1 | Animal models

All experiments involving animals followed experimental protocols approved by San Raffaele Hospital and Roswell Park Institute Animal Care and Use Committees. *Itgav* (α_V)-*floxed* mice: $Itgav^{f/+}$ mice of mixed C57BL6/129S4/FVB background (Lacy-Hulbert et al., 2007; McCarty et al., 2005) were mated to generate $Itgav^{f/f}$ or crossed with *Mpz*-Cre (P_0-Cre) transgenic mice of congenic C57BL6 background (Feltri, D'Antonio, Previtali, et al., 1999; Feltri, D'Antonio, Quattrini, et al., 1999) to generate $Itgav^{f/+}$; P_0-$Cre^{tg/+}$. $Itgav^{f/f}$ were then crossed with $Itgav^{f/+}$; P_0-$Cre^{tg/+}$ to produce $Itgav^{f/f}$; P_0-$Cre^{tg/+}$. Resulting offspring were of mixed background. $Itgav^{f/f}$ or $Itgav^{f/+}$ were used as controls. *Itga5/Itgav* (α_5/α_V)-*floxed mice*: *Itga5*-floxed mice, provided by van der Flier et al. (2010), were maintained in congenic C57BL6 background in our lab. We crossed $Itga5^{f/f}$ with $Itgav^{f/f}$; P_0-$Cre^{tg/+}$ to produce $Itga5^{f/+}$; $Itgav^{f/+}$; P_0-$Cre^{tg/+}$, which were then crossed with $Itga5^{f/f}$; $Itgav^{f/f}$ to produce $Itga5^{f/f}$; $Itgav^{f/f}$; P_0-$Cre^{tg/+}$. $Itga5^{f/f}$ and $Itgav^{f/f}$ were used as controls. Resulting offspring were of mixed background. *Itgb3* (β_3) mice: Male and female $Itgb3^{+/-}$-mice of congenic C57BL6 background were purchased from The Jackson Laboratory (B6.129S2-Itgb3^{tm1Hyn}/JSemJ, Stock No. 008819) and mated to produce $Itgb3^{-/-}$ mutants and $Itgb3^{+/+}$ controls. *Itgb8* (β_8) mice: $Itgb8^{-/-}$ mutants and $Itgb8^{+/+}$ controls of mixed C57BL6/129S4/ICR/CD1 background were described previously (Mobley et al., 2009). In all analyses, males and females were included, and only littermates or mice with the same parents were compared. PCR genotyping was performed in-house with phenol/chloroform-extracted DNA from tails or sciatic nerves, as previously described (Feltri, D'Antonio, Previtali, et al., 1999; Lacy-Hulbert et al., 2007; Mobley et al., 2009; van der Flier et al., 2010).

2.2 | Cell culture

All coculture experiments strictly contained only pure populations of SCs and dorsal root ganglia (DRG) neurons. *Purified rat SCs*: Purified populations of SCs (at >99.5% purity) were derived from Sprague–Dawley P3 rat sciatic nerves (Envigo or Taconic) using method in Brockes, Fields, and Raff (1979) and as performed in Feltri, Scherer, Wrabetz, Kamholz, and Shy (1992). Secondary SCs (stored in liquid N_2) were resuspended in SC media (DMEM, 10% fetal bovine serum [FBS], 2 μM forskolin, 2 mM L-glutamine, 2 ng/ml, Neuregulin-β1, 100 U/ml penicillin, and 100 μg/ml streptomycin [penn/strep]), plated on 100 mm culture dishes coated with 0.1 mg/ml poly-L-lysine (PLL) (Sigma-Aldrich), and maintained at 37°C in 5% CO_2 (37°/5%). *Purified rat DRG neurons*: Pure DRG neurons were achieved as described in Einheber, Milner, Giancotti, and Salzer (1993). DRGs were isolated from Sprague–Dawley embryonic day (E) 15.5 rat embryos, dissociated with 0.25% trypsin in DMEM for 45 min at 37°/5%, pelleted, then further disaggregated with 20 gentle

triturations in C-media (MEM, 10% FBS, 2 mM L-glutamine, 4 g/L D-glucose, 50 ng/ml nerve growth factor [NGF] [Harlan Bioproducts for Science]) supplemented with penn/strep. DRG suspension was then plated on 12 mm coverslips coated with 0.5 mg/ml rat collagen Type I (R&D Systems) at a density of 1.5 DRGs/coverslip. Coverslips were incubated at 37°/5%. After 24 hr, C-media were replaced by NB media (Neurobasal media, 2 mM L-glutamine, 4 g/L D-glucose, B27 Supplement 1X [Gibco], 50 ng/ml NGF) supplemented with 10 μM FUDR (Sigma-Aldrich) (NBF media) to eliminate endogenous, nonneuronal cells. After 48 hr, NBF media were replaced by NB media. DRG explants were maintained in alternating NBF/NB media for 2–3 cycles. These treatments resulted in pure DRG neurons devoid of all other cell types. *Mouse SC isolation* (*for SMAD4 analysis in α_V SCs and for real-time quantitative PCR [RT-qPCR] of α_5/α_V SCs*): Sciatic nerves were sampled from *Itgav*$^{f/f}$ and *Itgav*$^{f/f}$; *P*$_0$-*Cre*$^{tg/+}$ littermates or *Itga5*$^{f/f}$; *Itgav*$^{f/f}$ and *Itga5*$^{f/f}$; *Itgav*$^{f/f}$; *P*$_0$-*Cre*$^{f/f}$ littermates at P17 and placed in chilled Leibovitz's L-15 supplemented with penn/strep. Nerves were desheathed and teased under stereodissecting microscope. Teased nerves were dissociated in 0.25% DispaseII, 0.05% Type I collagenase, high-glucose DMEM overnight (O/N) at 37°C in 9% CO_2 (37°/9%). Next day, dissociated nerves were gently triturated, then 20 volumes of DMEM were added to hamper digestion. Suspension was filtered through 70 μm cell strainer. Cells were pelleted, gently resuspended in SC media, then plated on 12 mm coverslips or 35 mm dishes (previously coated with 0.1 mg/ml PLL (30 min room temperature [RT]), followed by 30 μg/ml laminin (Sigma-Aldrich L2020) O/N at 4°C) and incubated O/N at 37°/9%. For next 2 days, cells were washed with PBS to remove debris and replaced with new SC media. On the third day, fibroblasts were eliminated by incubating cells *with rat antimouseThy1.2* antibody (Ab) (AbD Serotec MCA1474) diluted in DMEM for 30 min at 37°/9%, followed by rabbit complement [1:500] (EMD Millipore 234400) for 40 min at 37/9%. Cells were washed, then maintained in SC media at 37°/9% for 2 days. Complement treatment was repeated to achieve maximal fibroblast removal.

2.3 | Competitive antagonist assay

Purified cultured rat SCs were washed 3x with PBS, trypsinized, pelleted, then gently resuspended in C-media with 20 gentle triturations. Antagonist peptides *iso*DGR (Curnis et al., 2006; Ghitti et al., 2012; Spitaleri et al., 2008), ac-*iso*DGR (Curnis et al., 2010), or negative control ARA peptides (200 μg/ml) were added to the SC suspension and incubated for 13 min at RT. Meanwhile, coverslips of purified rat DRG neurons were washed 3x with PBS. After 13 min, SC suspension (with peptides) was seeded onto DRG coverslips at a density of 20,000 SC/coverslip (200 μl drop/coverslip), then incubated for 3.5 or 16 hr at 37°/5%. Cocultures were then processed for immunostaining (see below). Five experiments were performed over 2 days for all conditions. To quantify SC length in Fiji/ImageJ, a line was drawn from tip to tip of bipolar SC (always going through nucleus), then measured. For multipolar SC, a line was drawn between the two longest observable tips (going through nucleus).

2.4 | Immunoblots

Cultured SCs, cultured DRG neurons, or SC/DRG cocultures were washed 3x with PBS to remove nonadherent entities, then lysed from the plate with lysis buffer (95 mM

NaCl, 25 mM Tris–HCl pH 7.4, 10 mM EDTA, 2% SDS, 1 mM Na_3VO_4, 1 mM NaF, Protease Inhibitor Cocktail [1:100] [Sigma-Aldrich]). Mouse sciatic nerves were sampled at indicated age, stripped of their epineurium (desheathed), snapfrozen, pooled, pulverized, then resuspended in lysis buffer. All lysates were boiled at 100°C for 5 min, then centrifuged at 14,000 rpm for 15 min at 16°C. Protein concentration was determined using BCA protein assay (Thermo Scientific). Homogenates containing 20 μg of protein were diluted in 4x Laemmli sample buffer (250 mM Tris–HCl pH 6.8, 8% SDS, 8% β-mercaptoethanol, 40% glycerol, 0.02% bromophenol blue, H_2O). Samples were boiled at 100°C for 5 min, centrifuged at 14,000 rpm for 2 min at RT, resolved on SDS-PAGE, then transferred to PVDF membranes. Membranes were blocked with 5% dry milk in 0.1% Tween-20/TBS (TBS-T) or 5% BSA in TBS-T for 1 hr shaking at RT, then incubated with primary Ab diluted in blocking solution O/N shaking at 4°C. The following primary Abs were used: *rabbit anti-α_V integrin* [1:1,000] (Cell Signaling #4711), *rabbit anti-β_3 integrin* [1:1,000] (Cell Signaling #4702), *rabbit anti-β_5 integrin* [1:1,000] (D24A5, Cell Signaling #3629), *rabbit anti-β_6 integrin* [1:1,000] (Proteintech 19695–1-AP), *rabbit anti-β_8 integrin* [1:5,000] (McCarty et al., 2005), *rabbit anti-α_5 integrin* [1:1,000] (EMD Millipore AB1928), *rabbit anti-Sox10* [1:1,000] (Cell Signaling #89356), *rabbit anti-GAPDH* (Sigma-Aldrich G9545), *rabbit anti-Calnexin* (Sigma-Aldrich C4731*), mouse anti-β-tubulin*. (Sigma-Aldrich T4026). Membranes were washed with TBS-T, then incubated with appropriate HRP-conjugated secondary Ab diluted in 1% dry milk/TBS-T or 1% BSA/TBS-T for 1 hr shaking at RT. ECL substrate (Pierce ECL, Thermo Fisher) was applied to membrane, then developed on autoradiography films (GE Healthcare). Immunoblots were quantified using Fiji/ImageJ. Specificity of the α_V and β_3 integrin Abs was tested and confirmed by short interfering RNA (siRNA)-mediated knockdown of α_V or β_3 in SCs (Supporting Information Figure S4c,e). Specificity of β_8 Ab was confirmed previously (McCarty et al., 2005; Mobley et al., 2009). For β_5 and β_6 integrin Abs, we exploited α_V's absence in DRG neurons and purposed these cells as negative controls as a way to infer the specific β_5 and β_6 bands in our immunoblots.

2.5 | siRNA-mediated knockdown of integrins in SCs

Purified cultured rat SCs were plated at a density of 500,000/well on a six-well plate coated with 0.1 mg/ml PLL and incubated in SC media at 37°/5% O/N. SCs were transfected when 40% confluent (next day) with 33 nM of four siRNA targets against integrin subunit α_V (Thermo Scientific J-091817–09, 10, 11, and 12) or β_3 (Thermo Scientific J-097040–05, 06, 07, and 08) using Lipofectamine 2000 (Thermo Fisher), then incubated for 6 hr at 37°/5%. Cells were thereafter maintained in SC media at 37°/5% for 72 hr. To verify protein knockdown, SCs were washed, lysed from the plate, then processed for immunoblot as described above. To seed SCs onto DRG neurons, SCs were washed 3x with PBS, trypsinized, pelleted, then resuspended in C-media with 20 gentle triturations. SC suspension was seeded onto pure rat DRG coverslips (400 μl/coverslip, at a density of 20,000 SC/coverslip), then incubated for 3.5 or 24 hr at 37°/5%. Cocultures were then processed for immunoblot or immunostaining. The following number of experiments was performed over 3 days: scrambled = 8, si-$\alpha_V^{\#2}$ = 8, si-$\alpha_V^{\#2}$ = 6, si-$\alpha_V^{\#2}$ = 4. *siRNA-treated SCs on FN*: 12 mm coverslips were coated with 10 μg/ml FN (Sigma-Aldrich F2006) diluted in PBS and stored O/N at 4°C. siRNA-treated SCs were washed 3x with PBS, trypsinized, pelleted, then resuspended in SC media with 20 gentle triturations. SC suspension was

plated on dried FN coverslips at a density of 40,000 SC/coverslip (80 μl drop/coverslip), then incubated for 3.5 hr at 37°/5%. Cells were then processed for immunostaining (see below). *Quantification of SC length in 3.5 hr cocultures*: same as competitive antagonist assay. *Quantification of cell number in 24 hr cocultures*: Each field was imaged under ×10 objective of Leica DM6000B microscope. All SCs in the field were associated with axons. Only SC DAPI was quantified in Fiji/ImageJ.

2.6 | Immunostaining

Immunostaining of cultured SC or sciatic nerves: OCT-embedded sciatic nerves were sliced into 8 μm-thick sections with Cryostat and stored in −20°C for no more than 48 hr prior to immunostaining. Sections were thawed for 5 min, then submerged in PBS for 5 min. Cultured cells were washed 3x with PBS. Cells or nerve sections were fixed with 4% paraformaldehyde (PFA)/PBS for 10 min RT, permeabilized with 0.2% Triton-X/PBS for 10 min RT, then incubated in blocking solution for 1 hr RT. Cells or nerves were incubated O/N at 4°C with primary Abs diluted in blocking solution. The following primary Abs were used: *rabbit anti-S100* [1:150–1:200] (Dako Z0311), *goat anti-SOX10* [1:400] (R&D Systems AF2864), *rabbit anti-SMAD4* [1:150] (Proteintech 51069–2-AP), *rabbit anti-Ki67* [1:400] (Cell Signaling #9129), *rabbit anti-phospho-Histone H3* (*PH3*) [1:400] (EMD Millipore 06–570). Cells or nerves were washed, incubated with appropriate secondary Ab diluted in blocking solution for 1 hr at RT, washed, stained with DAPI [1:10,000] (Sigma-Aldrich D9542) for 3 min RT, washed, mounted with Vectashield, then sealed. *Immunostaining of co−/cultured SC for* α_V: Cultured SCs were dyed with CellTracker fluorescent green probe (Invitrogen C7025), following manufacturer's protocol. Dyed SCs were then seeded on DRGs for experiment (as described above). Cocultures were washed to remove nonadherent entities, then permeabilized with chilled methanol for 1.5 min at RT. Methanol was thoroughly aspirated, then cells were washed, permeabilized with 0.2% Triton-X/PBS for 10 min RT, washed, incubated in blocking solution (20% FBS, 2% BSA, 0.1% Triton-X, PBS) for 2.5 hr at RT, then washed again. Cells were then incubated for 1.5 hr at RT with primary Ab diluted in blocking solution. The following Abs were used: *rabbit anti-*α_V *integrin* [1:150] (EMD Millipore AB1930), *rat or chicken anti-Neurofilament* [1:500–1:1,000] (EMD Millipore MAB5448, Biolegend 822701), mouse *anti-tubulin* [1:200] (Sigma-Aldrich T4026). Cells were washed, then incubated with secondary Ab diluted in PBS for 1 hr RT. Remaining steps were same as above. *Teased fiber immunostaining*: Fixed fibers were submerged in chilled acetone for 5 min, then incubated in blocking solution (5% fish skin gelatin, 0.5% Triton-X100, PBS) for 1 hr RT. Remaining steps were same as general immunostaining above. Primary Abs used: *rabbit anti-*K_V*1.1* (Alomone Labs APC-009), mouse anti-*Nav Pan* (Sigma-Aldrich S8809). *Ki67 and PH3 immunostaining*: Two nerves per animal, two animals per genotype were analyzed. The whole length of sampled P3 nerve (~3 mm) was immunostained, imaged, and quantified. All immunostainings were imaged using Confocal Leica TCS SP5 II microscope and Leica software. All images are Z-series projection comprised of 0.5–1 μm slices.

2.7 | SMAD4 analysis in SCs

TGFβ stimulation was performed as described (D'Antonio et al., 2006). Briefly, SCs isolated from *Itgav*$^{f/f}$ or *Itgav*$^{f/f}$; *P*$_0$-*Cre*$^{tg/+}$ mice were treated with recombinant mouse

TGFβ1 (10 ng/ml) (R&D Systems 7666-MB-005) for 30 min at 37°/5%, washed, fixed with 4% PFA, then immunostained and imaged as described above. For *Itgav*$^{f/f}$, 2,391 SCs were quantified from five animals. For *Itgav*$^{f/f}$ and *P*$_0$-*Cre*$^{tg/+}$, 1,955 SCs were quantified from five animals. SCs from each animal were plated in duplicate.

2.8 | Real-time quantitative PCR

RNA was isolated from purified SCs derived from desheathed sciatic nerves of *Itga5*$^{f/f}$; *Itga5*$^{f/f}$ or *Itga5*$^{f/f}$; *Itga5*$^{f/f}$; *P*$_0$-*Cre*$^{tg/+}$ postnatal day (P)17 and P6 mice using RNeasy Plus Micro Kit (Qiagen) and TRIzol (Thermo Fisher), respectively. cDNA was synthesized using Super-Script III Reverse Transcriptase kit (Life Technologies). Expression levels of α_5 integrin were measured using Taqman Gene Expression Assay kit (Applied Biosystems, TaqMan Assay ID Mm00439797_m1). 18S rRNA was used as endogenous control (Applied Biosystems, TaqMan Assay ID Hs99999901_s1).

2.9 | Morphological analysis

Mutant and control littermates were euthanized at the age indicated. The sciatic nerve segment was sampled from approximately the same position for every age cohort. Routine semithin and ultrathin (electron micrograph [EM]) analyses were performed as described (Quattrini et al., 1996). Briefly, sciatic nerves were fixed in 2% buffered glutaraldehyde, then postfixed in 1% osmium tetroxide. After alcohol dehydration, nerves were submerged in propylene oxide, then in a 1:1 mixture of Epon-propylene oxide. Nerves were embedded in 100% Epon, and resin was allowed to polymerize. Semithin transverse sections were sliced 0.5-μm-thick using Leica UC7, stained with 2% toluidine blue, then examined by light microscopy with Leica DM6000B. EM transverse sections were sliced 700–900-Å-thick using Leica UC7, stained with uranyl acetate and lead citrate, then examined with electron microscope (model FEI BioTwin). Analyzed sections were sliced from the distal end of embedded sciatic nerve. Images acquired from semithins and EMs were nonoverlapping and comprehensive. To determine myelin thickness, the G-ratio (axon diameter/fiber diameter, where fiber = axon + myelin) was quantitated manually from EMs. In Fiji/ImageJ, a segmented line was drawn along the border of each axon, then its circumference was measured. The process was repeated for the whole fiber (axon including myelin), drawing the segmented line along the outer myelin border. Diameter was extracted using $d = C/\pi$. Axon diameter was divided by the fiber diameter to obtain G-ratio. Number of myelinated fibers was counted per EM field of view, then averaged. Any axon with surrounding myelin, regardless of thickness, was considered myelinated. Number of axon/SC units in 1:1 relationship was counted per EM field of view, then averaged. Any axon ensheathed (but not myelinated) by an individual SC was considered 1:1.

2.10 | Internodal length

The length between two internodes was measured from teased sciatic nerve fibers sampled from adult α_V (P33) or α_5/α_V (P152) mice. Teased sciatic nerve fibers were prepared as previously described (Occhi et al., 2005). Briefly, control and mutant nerves were dissected, then immersed in chilled 4% PFA for 30 min. Fixed nerves were stored in PBS at 4°C until teasing (within 1 week). After epineurium removal, nerve fibers were gently teased apart with fine tungsten pins on 3-aminopropyltriethoxy-sylane-treated slides. All teasing steps

were done under a stereodissecting microscope. Teased fibers were then allowed to dry on slides for at least 4 hr RT. Fibers were processed for $K_V1.1$ and PanNaV immunostaining and imaged as described above. Length of internodes was measured in Fiji/ImageJ. A segmented line was drawn from one (PanNaV) node to the next, then length was measured.

2.11 | Nerve crush

Nerve crush was performed on adult mice using aseptic technique under a biobubble hood. Mice were anesthetized with isofluorane, and eyes were lubricated. While mouse laid flat on its dorsal side, the region of intended crush was shaved and cleaned with betadine and ethanol. On one leg, a small incision was made in the skin and muscle above the approximate position of sciatic nerve. Once nerve was exposed, any membranous ties to the muscle were severed using small scissors. A pair of straight serrated forcep clamps was dipped in liquid N_2 for 2 s, then nerves were tightly compressed with chilled clamps for 20 s. Crush site was marked with bromophenol blue powder, and process was repeated a second time on same crush site. Nerve was crushed, but not severed. Position of crush was approximately the same for every cohort. Other leg was unoperated. Injured skin was closed with surgical glue, then buprenorphine was administered subcutaneously as post-operatory analgesia. Animals were monitored daily after surgery and analgesics were administered as necessary. Then, 15 or 30 days postcrush, three segments of the operated nerve were sampled: (a) the segment proximal to the crush site, (b) the crush site, and (c) the segment distal to the crush site. Sciatic nerve from unoperated leg was also sampled. Nerves were prepared for semithin sectioning (as described above). Sections of all segments were analyzed, but only distal segments were quantified. Number of myelinated fibers was counted per semithin field of view, then averaged. Ages of animals used: α_V T15, 4 months; α_V T30, 3 months; α_5/α_V T15, 5 months; α_5/α_V T30, 4 months.

2.12 | Image acquisition and statistics

Researcher was blind to the genotype during image acquisition and quantification. Images acquired were nonoverlapping. For antagonist and siRNA coculture experiments, areas of coverslip too congested with neurons were neither imaged nor included in quantification. All statistics were done in GraphPad Prism (ver 7.0). Specific analysis is stated in the legend. ****$p < .0001$, ***$p < .001$, **$p < .01$, *$p < .05$, ns = not significant ($p > .05$). All images are representative fields.

3 | RESULTS

3.1 | Antagonists of RGD-binding integrins hinder extension of SCs on axons in vitro

Previously it was shown that RGD peptides inhibit the process extension of SCs plated on FN (Milner, Wilby, et al., 1997). To determine if RGD-binding integrins are also involved in axo-glial interactions, we pretreated WT SCs with competitive antagonists against RGD-binding integrins, plated them on untreated WT DRG neurons, and assessed their interaction. SCs were pretreated with either (a) ARA, a cyclic Ala-Arg-Ala nonspecific peptide (negative control), (b) *iso*DGR, a cyclic *iso*Asp-Gly-Arg peptide with high affinity for $\alpha_V\beta_3$, or (c) ac-*iso*DGR, a cyclic, acetylated form of *iso*DGR with similar affinities (thus less selective) for several RGD-binding integrins.

After 3.5 hr, ARA-treated SCs attached to axons and generated lengthy processes that aligned with one axon or contacted multiple axons (Figure 1a); they appeared like untreated SCs at 3.5 hr (Supporting Information Figure S1d). In contrast, treatment with *iso*DGR or ac-*iso*DGR hindered process extension: SCs attached to axons, but were visibly shorter and more stunted compared to ARA-treated SCs (Figure 1b–d). Those with little to no protrusions (stunted) and those with only short processes significantly increased in *iso*DGR and ac-*iso*DGR cohorts (Figure 1e). Furthermore, those with long processes significantly decreased. These demonstrate that RGD-binding integrins are involved early in axo-glial interactions and suggest the association of axons and SCs may be in part RGD dependent.

Since *iso*DGR- and ac-*iso*DGR-treated SCs in cocultures of 3.5 hr resembled untreated SCs in cocultures of 1 hr (Supporting Information Figure S1b), we asked whether the antagonist peptides simply delayed or completely arrested process extension. In prolonged cocultures, *iso*DGR and ac-*iso*DGR cohorts did lengthen, though not to the same span as ARA controls (Supporting Information Figure S1e–g), indicating delay, not blockade.

3.2 | α_V-containing integrins are expressed during radial sorting in vivo

We next characterized the expression of α_V-containing integrins ($\alpha_V\beta_3$, $\alpha_V\beta_5$, $\alpha_V\beta_6$, $\alpha_V\beta_8$) in SCs. α_V-containing integrins constitute the majority of RGD-binding integrins (Supporting Information Figure S1a) in addition to $\alpha_5\beta_1$ integrin, whose expression in peripheral nerves was characterized previously (Lefcort, Venstrom, McDonald, & Reichardt, 1992), and $\alpha_8\beta_1$ integrin, which is not expressed in an RNA database from developing sciatic nerves (D'Antonio et al., 2013). Integrin β_5, β_6, and β_8 are known to dimerize exclusively with the α_V integrin subunit, whereas integrin β_3 can dimerize with the α_V or α_{IIb} subunits, the latter's expression being limited to platelets and megakaryocytes (Phillips, Charo, & Scarborough, 1991).

By immunoblot, we detected α_V proteins in developing sciatic nerves (Figure 2a,b). α_V levels were high during radial sorting and the onset of myelination (P3–P5), progressively fell at the peak of myelination (P15) and after myelination (P28), and were relatively low in adults (2 months), which suggested α_V-containing integrins may have a role during radial sorting. We also detected the known partners of the integrin subunit α_V: β_3, β_5, β_6, and β_8. Except for subunit β_5, their levels generally declined throughout development. Because SCs are not the only cell type in the sciatic nerve, we also investigated if α_V and its β partners were expressed in purified SCs and DRG sensory neurons. By immunoblot, we detected integrins α_V, β3, β5, β6, and β8 in purified SCs, but only β5 integrin was also expressed in purified DRG neurons (Figure 2c). Coculturing DRGs and SCs did not increase expression of these integrins, with the possible exception of β8 (Figure 2c,d). These data provide evidence that SCs express RGD-binding integrins that contain subunit α_V and that they are present at relatively high levels during development.

3.3 | SCs deficient in the α_V integrin subunit elongate less in vitro

To confirm that the effect of the antagonist peptide was mediated by α_V integrin heterodimers, we performed siRNA knockdown of the α_V integrin subunit (si-$\alpha_V^{\#2}$, -$\alpha_V^{\#3}$, or -$\alpha_V^{\#4}$) in SCs (Figure 3e), then plated them on WT DRG neurons. After 3.5 hr,

α_V-silenced SCs elongated less on axons compared to SCs transfected with scrambled siRNA (negative control) (Figure 3a–d). Average SC length in all silenced cohorts decreased (Figure 3f), because significantly more SCs were stunted, more formed short processes, and fewer elaborated long processes (Figure 3g). α_V-silenced SCs also eventually lengthened in prolonged cocultures (Supporting Information Figure S3a–f), indicating elongation delay. In effect, depleting SCs of all α_V-containing integrins phenocopied *iso*DGR- and ac-*iso*DGR-treated SCs, suggesting that α_V heterodimers were the main mediators.

We hypothesized $\alpha_V\beta_3$ integrin to be the relevant receptor because *iso*DGR peptides (which have strong affinity for $\alpha_V\beta_3$) and ac-*iso*DGR peptides (which do not discriminate between integrins $\alpha_V\beta_3$, $\alpha_V\beta_5$, $\alpha_V\beta_6$, $\alpha_V\beta_8$, or $\alpha_5\beta_1$) elicited comparable effects. However, silencing subunit β_3 did not impact extension of SC on axons (Supporting Information Figure S4a,b), suggesting that β_3-associated integrins like $\alpha_V\beta_3$ are nonessential for extension along axons. Moreover, α_V protein levels remained stable despite marked reduction of the subunit β_3 protein (Supporting Information Figure S4c–f), suggesting other α_V heterodimers may still be functioning in the absence of $\alpha_V\beta_3$ integrin. Together, these suggest SCs can utilize multiple α_V-containing integrins for proper lamellipodia extension toward axons.

3.4 | α_V-containing integrins localize to the tips of SC protrusions

We next determined the localization of α_V integrin when SCs contact axons by immunocytochemistry. We first confirmed the specificity of anti-α_V antibodies by plating scrambled and α_V-silenced SCs on FN-coated coverslips, then immunostained for α_V. After 3.5 hr on FN, α_V-silenced SCs spread and elaborated lamellipodia, with no obvious morphological dissimilarities from controls (Figure 4a,b), demonstrating that α_V integrin is nonessential for forming SC protrusions on FN. The tips of protruding lamellae were strongly immunoreactive in control SCs (Figure 4a); this specific signal and the diffused staining diminished in α_V-silenced SCs (Figure 4b). In 3.5 hr cocultures, α_V was enriched at the terminal ends of the SC that were contacting the axon (Figure 4c,d). Conversely, α_V-silenced SCs (Figure 4e), including the few able to elongate (Figure 4f), were not immunoreactive to α_V. These data illustrate that α_V integrin localizes at axon-associated SC extremities within few hours of coculture.

3.5 | SC-specific deletion of subunit α_V does not affect myelination in vivo

To determine if α_V-containing integrins play a role in myelination in vivo, we deleted subunit α_V by crossing homozygous *Itgav*$^{f/f}$ floxed mice with hemizygous mice carrying the *P*$_0$-*Cre* transgene. The P_0 promoter drives Cre expression primarily in SCs beginning at E13.5, producing conditional KO (cKO) mice (*Itgav*$^{f/f}$; *P*$_0$-*Cre*) with α_V deleted specifically in SCs (Figure 5a). Unlike embryonic and neonatal-lethal whole body *Itgav*$^{-/-}$ mice (McCarty et al., 2002), SC cKOs were viable and survived to late adulthood without obvious behavioral defects. EM cross sections of P3, P5, and P10 sciatic nerves showed no evidence of improper radial sorting or myelination in cKOs (Figure 5b–g). Myelin thickness (G-ratio) (Figure 5j,k,m,n), the density of myelinated fibers (Figure 5l,o), the density of 1:1 axon/SC units (Figure 5p), basal lamina formation (Figure 5h), nodal organization (Figure 5q), and internodal length (Figure 5r) were comparable to controls. Furthermore, myelination in whole body *Itgb3*$^{-/-}$ and *Itgb8*$^{-/-}$ mice was normal (Figure 5s–u,v–y, respectively).

Together, these data show that α_V-containing SC integrins are nonessential for in vivo myelination.

α_V integrin heterodimers bind to the RGD-bearing LAP (latent-associated peptide) fragment of the TGFβ complex to activate the TGFβ pathway (Henderson et al., 2013), and αVβ8 integrin in nonmyelin forming SCs maintain the bone marrow niche by regulating the activation of TGF-β receptors (Yamazaki et al., 2011). Furthermore, since disrupting TGFβ signaling in SCs can lead to reduced proliferation without affecting myelination (D'Antonio et al., 2006), we hypothesized that cell proliferation and TGFβ signaling may be altered in cKO SCs. However, cell proliferation was normal in cKO P3 sciatic nerves (Figure 6a–f), and mutant SCs isolated from cKO nerves properly shuttled SMAD4 into the nucleus upon TGFβ1 stimulation (Figure 6g–r).

3.6 | SC-specific double deletion of the integrin subunits α_5 and α_V does not impact myelination in vivo

Compensation or functional overlap by other RGD-binding integrins could explain why α_V cKO had no phenotype. Numerous reports from other cell types demonstrating that α_5 and α_V integrins cooperate, compensate each other's loss, or functionally overlap (Bharadwaj et al., 2017; Charo, Nannizzi, Smith, & Cheresh, 1990; Turner, Badu-Nkansah, Crowley, van der Flier, & Hynes, 2015; van der Flier et al., 2010; Yang et al., 1999; Yang & Hynes, 1996) led us to hypothesize that integrin α_V and α_5 may be redundant. Deletion of *Itga5* specifically in SCs under the control of P_0-Cre, does not perturb myelination (data not shown). We therefore generated *Itga5*$^{f/f}$; *Itgav*$^{f/f}$; *P*$_0$-*Cre* conditional double knockout (cdKO) mice (Figure 7a–d, Supporting Information Figure S5a). As confirmed by immunoblot, integrin α_V proteins diminished in cdKO P10 nerves compared to controls (Figure 7a). We did not detect a decrease in α_5 protein in cdKO nerves by immunoblot (data not shown), despite genotypic confirmation that *Itga5* recombined in sciatic nerves (Figure 7b). Unexpectedly, RT-qPCR analysis showed that the relative expression of integrin α_5 in cdKO nerves increased compared to controls (Figure 7c). This increase must be attributable to endoneurial cells other than SC, because we saw a marked reduction in relative expression of integrin α_5 in isolated cdKO SCs by RT-qPCR (Figure 7d).

cdKO mice survived to late adulthood and behaved normally like controls. EM cross sections of cdKO nerves did not display obvious defects in radial sorting or myelination at P3, P10, or P28 (Figure 7e–j). Average G-ratios (Figure 7k,m), nodal organization (Figure 7o,p), and internodal length (Figure 7q) at P3 and P10 were similar to controls. However, the G-ratio distribution (as a function of axon diameter) in P10 cdKO had a slight but significant slope downshift relative to control (Figure 7l,n), suggesting that large fibers may have thicker myelin in cdKO nerves. Nevertheless, these data overall show that α_5- and α_V-containing integrins are nonessential for in vivo myelination.

3.7 | Remyelination after nerve crush proceeds in the absence of the integrin subunits α_5 and α_V

Several papers have proposed that RGD-based axo-glial interactions may be important for the remyelination process after nerve injury (Akassoglou, Akpinar, Murray, & Strickland,

2003; Akassoglou, Yu, Akpinar, & Strickland, 2002; Chernousov & Carey, 2003; Liu, Martinez, Durand, Wildering, & Zochodne, 2009; Qian et al., 2018; Rafiuddin Ahmed & Jayakumar, 2003; Zheng et al., 2015). To determine if α_5 or α_V integrins play a role in nerve degeneration, regeneration, or remyelination, we performed nerve crush on α_V integrin cKO and α_5/α_V integrin cdKO adult sciatic nerves, then examined axon regeneration and remyelination 15 and 30 days postcrush (T15 and T30, respectively). Injured nerves sampled from α_V integrin cKO (Figure 8a,c) or α_5/α_V integrin cdKO mice (Figure 8b,d) were morphologically similar to their respective controls, showing a similar number of axons and myelinated fibers and similar myelin thickness at both times, suggesting that α_5- and α_V-containing SC integrins are nonessential for nerve regeneration after crush.

4 | DISCUSSION

During development, SCs extend their processes to contact, sort, and myelinate axons. In vitro, we found that α_V integrins, a group that binds RGD-bearing ligands, localize in SC to specific sites of contact with axons and contribute to the extension of the process.

The integrin α_V subunit is expressed by western blot in early stages of nerve development when SCs are actively engaging axons to sort and myelinate them. We were unable to show the in vivo expression of α_V integrins by immunostaining because we could not validate the specificity of the anti-α_V antibody on tissue sections or teased fibers (data not shown). This is surprising, given that we could detect specific staining of α_V integrin in culture, and could be due to upregulation of α_V integrin on the more rigid and stiff environment of cultures. However, we believe that α_V integrin expression detected by western blot can be mainly attributable to SCs, because SC-specific ablation in vivo results in major reduction of the protein in whole nerve immunoblots, and we do not detect α_V integrin protein in cultured purified DRG neurons or axons. Our results are consistent with previous reports showing cultured SCs express the integrin subunits α_V, β_3, β_5, β_6, and β_8 (Chabas et al., 2013; Milner, Wilby, et al., 1997; Poitelon et al., 2015). Together with subunit β_1, a key SC integrin (Feltri et al., 2002), SCs can potentially form all five α_V integrin heterodimers. Of them, integrin $\alpha_V\beta_6$ may be the least likely to participate in the myelination process because of its low expression in vivo. However, it might participate in injury or disease, as SC β_6 localizes to the injury zone of transected nerves (Liu et al., 2009) and is differentially upregulated in severely amyelinated nerves (Poitelon et al., 2016). Integrins $\alpha_V\beta_3$ and $\alpha_V\beta_8$, on the other hand, could have distinct roles in development. We found that expression of the integrin subunits β_3 and β_8 are dynamic and developmentally regulated. It echoes the dynamic expression of α_V-associated β subunits in oligodendrocytes, which is postulated to reflect an integrin switching ($\alpha_V\beta_1$-$\alpha_V\beta_3$-$\alpha_V\beta_8$-$\alpha_V\beta_5$) in oligodendrocytes during development (Blaschuk et al., 2000; Milner et al., 1996; Milner & Ffrench-Constant,1994; Milner, Frost, et al., 1997).

Blocking or silencing integrin α_V in vitro impairs process extension, and as a result, many SCs assume a rounded, stunted morphology. Diminishing only integrin $\alpha_V\beta_3$ has no effect, but antagonistic inhibition of integrin $\alpha_V\beta_3$, $\alpha_V\beta_5$, $\alpha_V\beta_6$, $\alpha_V\beta_8$, and $\alpha_5\beta_1$ by ac-*iso*DGR and knockdown of all possible α_V heterodimers do reveal a loss-of-function in vitro. It is possible that RGD-binding integrins not directly tested by our analyses participate in

this process. Other β_1-containing integrins do not bind RGD primarily, but are capable of binding RGD or an RGD-related motif (Bazigou et al., 2009; Ruoslahti, 1996). Also, deletion of all β_1 integrins in SCs cause severe radial sorting defects (Feltri et al., 2002).

Surprisingly, conditional mutant mice lacking integrins α_V are normal, and α_5 integrin does not compensate for α_V integrin deficiency, despite the many papers postulating a possible role for these integrins in SC-axon interactions during myelination and remyelination (Akassoglou et al., 2002; Akassoglou et al., 2003; Chernousov & Carey, 2003; Liu et al., 2009; Qian et al., 2018; Rafiuddin Ahmed & Jayakumar, 2003; Zheng et al., 2015). We show that α_V and α_5 integrins are not required for radial sorting, myelination, and remyelination after injury in vivo. In our case, the coculture system may have been more permissive to reveal a phenotype because, unlike in vivo, seeded SCs are synchronized and associated with axons simultaneously. With a time-sensitive in vitro phenotype (delay), this becomes a major limitation in vivo because SCs in the nerve are asynchronized and associate with axons at different times. Similar discrepancies between the presence of phenotype in DRG coculture systems, but absence of phenotype in vivo has been observed previously in various reports (Eshed et al., 2005; Li et al., 1994; Owens, Boyd, Bunge, & Salzer, 1990; Owens & Bunge, 1989, 1990, 1991), and may be due to the lack of compensatory mechanisms in vitro, to the more simplified cellular system, or to the different 3D arrangements of DRGs versus peripheral nerves.

The possibility of compensation by other receptors in vivo likely explains the lack of phenotype. Many more cellular molecules are present in the nerve compared to our coculture environment, and any receptor capable of binding RGD motifs could potentially contribute; we propose β_1-containing integrins such as $\alpha_8\beta_1$ (which binds to RGD motif) or $\alpha_4\beta_1$ (which binds to RGD-related motif) (Humphries, 2006) as potential candidates. In endothelial cells lacking both α_V and α_5, $\alpha_4\beta_1$ relocalizes to focal adhesions formerly occupied by α_V and α_5 (van der Flier et al., 2010). Assessing any integrin expression changes between control, α_V cKO, and α_5/α_V cdKO transcriptomes could help identify contributing integrins, and the coculture system would be a good and practical first step in which to test these all these potential integrins using peptidomimetics, next generation small molecule inhibitors (Reed et al., 2015), or gene knockdowns of central integrins. Nonintegrin molecules may also compensate, especially in light of integrins' ability to cross talk and cosignal with growth factor receptors and several molecules along signal transduction pathways (Schwartz & Ginsberg, 2002). We show that RGD-binding integrins are involved in axo-glial interactions in vitro; identifying the potential axonal ligands of these integrins could also lead to the identification of the compensating molecules in question.

Perturbation of the same integrins between different systems and cell types have often resulted in discrepancies (Hynes, 2002a) perhaps because integrins are so versatile in their interactions, that their functions are context-specific and therefore somewhat unpredictable. in vitro testing coupled with in vivo validations should help define their context-specific roles. Additionally, recent papers show that a precise mechanism elicited by nonsense mutations in vivo triggers a complex compensatory response that upregulates many genes with sequence similarity to the deleted one (El-Brolosy et al., 2019; Ma et al., 2019).

This mechanism masks defects in vivo. Many KO or Cremediated mutants are designed to generate frame-shift and stop codon which commonly elicit a nonsense-mediated decay response, and even if we have not formally documented it in our mutants, the design of the α_V and α_5 integrin animals both results in premature stop codons, and thus a nonsense mutation, indicating that this mechanism may be in place.

Interestingly, we recently found that α_V integrin, along with important integrin and promyelinating genes, is significantly downregulated in mice completely arrested in radial sorting (Poitelon et al., 2016). This could indicate α_V integrin is indeed a participant in radial sorting in vivo. These mice lack key mechanotransduction regulators YAP and TAZ in SCs, and it has been shown in other cell types that *Itgav* is a target of YAP (Nardone et al., 2017). Intriguingly, MDCK epithelial cells lacking α_V integrin assume a “roundish” morphology and fail to respond to substrate rigidity, which is indicative of impaired mechanotransduction (Teräväinen et al., 2013). It is thus conceivable that SC mechanosensing involves α_V integrins. The dissimilarity of the nerve and coculture mechanical environments may have also contributed to our in vitro and in vivo discrepancies in detecting α_V integrin expression and function. The ECM and the other cells surrounding SCs in vivo could impose a differential mechanical stimuli on SCs compared to the neurons and substrate in the coculture (Belin, Zuloaga, & Poitelon, 2017).

Despite possible overlap or compensation, we define the precise step in which SC α_V integrin exerts its function, at least in vitro. For one, α_V integrin is not required for axon recognition or adhesion, given that impaired SCs can still anchor themselves onto axons (not substrate) and that a comparable number of impaired and control SCs do adhere. Instead, α_V integrin seems to participate in the early phases of process extension, as many α_V-silenced or antagonist-treated SCs in short-term cocultures are stunted and many do not reach the lengths of their control counterparts. This aligns with Milner, Wilby, et al.’s (1997) findings, who demonstrated that SC migration is hindered by RGD peptides. Since process extension is an inaugural step of cell migration, it is possible that this precise step is perturbed.

Glial α_V integrin has mostly been studied within the context of ECM interactions, but here we show that SC α_V integrin may possibly function independently of ECM ligands and that its role could in part be axon dependent. SCs plated on FN appear unaffected by depletion of all α_V heterodimers, yet axon-related SCs become disturbed, suggesting axons have a unique impact on SC α_V integrin. We propose that SC α_V interacts with axonal molecules and functions *ad*-axonally. There are a few other examples of α_V integrins mediating cell–cell interaction. Interestingly, α_V integrins have been shown to bind directly to L1 (Montgomery et al., 1996), Neuregulins (Ieguchi et al., 2010), and ADAM molecules (Nath et al., 1999; Zhou, Graham, Russell, & Croucher, 2001). Nrg1-Type III and ADAM22 are essential for myelination (Ozkaynak et al., 2010; Taveggia et al., 2005) and α_V integrins could modulate the interaction between these molecules and their obligate receptors, Erb2/3 and Lgi4 (Bermingham et al., 2005), respectively.

Supplementary Material

Refer to Web version on PubMed Central for supplementary material.

ACKNOWLEDGMENT

The authors would like to thank Flavio Curnis for RGD peptides. This work was funded by National Institute of Health (NIH) under grant NINDS-R01NS045630 (to M. L. F.).

Funding information

National Institute of Health, Grant/Award Number: NIH-NINDS R01NS045630

DATA AVAILABILITY STATEMENT

The data that support the findings of this study are available from the corresponding author upon reasonable request.

REFERENCES

Akassoglou K, Akpinar P, Murray S, & Strickland S (2003). Fibrin is a regulator of Schwann cell migration after sciatic nerve injury in mice. Neuroscience Letters, 338(3), 185–188. 10.1016/S0304-3940(02)01387-3 [PubMed: 12581827]

Akassoglou K, Yu WM, Akpinar P, & Strickland S (2002). Fibrin inhibits peripheral nerve remyelination by regulating Schwann cell differentiation. Neuron, 33(6), 861–875. [PubMed: 11906694]

Aumailley M, Gerl M, Sonnenberg A, Deutzmann R, & Timpl R (1990). Identification of the Arg-Gly-Asp sequence in laminin A chain as a latent cell-binding site being exposed in fragment P1. FEBS Letters, 262(1), 82–86. [PubMed: 2318314]

Bazigou E, Xie S, Chen C, Weston A, Miura N, Sorokin L, … Makinen T (2009). Integrin-alpha9 is required for fibronectin matrix assembly during lymphatic valve morphogenesis. Developmental Cell, 17(2), 175–186. 10.1016/j.devcel.2009.06.017 [PubMed: 19686679]

Belin S, Zuloaga KL, & Poitelon Y (2017). Influence of mechanical stimuli on Schwann cell biology. Frontiers in Cellular Neuroscience, 11, 571–511. 10.3389/fncel.2017.00347

Benninger Y, Thurnherr T, Pereira JA, Krause S, Wu X, Chrostek-Grashoff A, … Relvas JB (2007). Essential and distinct roles for cdc42 and rac1 in the regulation of Schwann cell biology during peripheral nervous system development. Journal of Cell Biology, 177(6), 1051–1061. 10.1083/jcb.200610108

Bermingham JR, Shearin H, Pennington J, O'Moore J, Jaegle M, Driegen S, … Meijer D (2005). The claw paw mutation reveals a role for Lgi4 in peripheral nerve development. Nature Neuroscience, 9(1), 76–84. 10.1038/nn1598 [PubMed: 16341215]

Berti C, Bartesaghi L, Ghidinelli M, Zambroni D, Figlia G, Chen Z-L, … Feltri ML (2011). Non-redundant function of dystroglycan and β1 integrins in radial sorting of axons. Development, 138(18), 4025–4037. 10.1242/dev.065490 [PubMed: 21862561]

Bharadwaj M, Strohmeyer N, Colo GP, Helenius J, Beerenwinkel N, Schiller HB, … Müller DJ (2017). αV-class integrins exert dual roles on α5β1 integrins to strengthen adhesion to fibronectin. Nature Communications, 8, 14348. 10.1038/ncomms14348

Blaschuk KL, Frost EE, & Ffrench-Constant C (2000). The regulation of proliferation and differentiation in oligodendrocyte progenitor cells by alphaV integrins. Development, 127(9), 1961–1969. 10.1002/jnr.490270319 [PubMed: 10751184]

Brockes JP, Fields KL, & Raff MC (1979). Studies on cultured rat Schwann cells. I. Establishment of purified populations from cultures of peripheral nerve. Brain Research, 165(1), 105–118. 10.1016/0006-8993(79)90048-9 [PubMed: 371755]

Cardwell MC, & Rome LH (1988). RGD-containing peptides inhibit the synthesis of myelin-like membrane by cultured oligodendrocytes. Journal of Cell Biology, 107(4), 1551–1559. 10.1083/jcb.107.4.1551

Chabas J-F, Stephan D, Marqueste T, Garcia S, Lavaut M-N, Nguyen C, … Feron F (2013). Cholecalciferol (vitamin D3) improves myelination and recovery after nerve injury. PLoS One, 8(5), e65034–e65015. 10.1371/journal.pone.0065034 [PubMed: 23741446]

Charo IF, Nannizzi L, Smith JW, & Cheresh DA (1990). The vitronectin receptor alpha v beta 3 binds fibronectin and acts in concert with alpha 5 beta 1 in promoting cellular attachment and spreading on fibronectin. Journal of Cell Biology, 111(6), 2795–2800. 10.1083/jcb.111.6.2795

Chernousov MA, & Carey DJ (2003). $\alpha_V\beta 8$ integrin is a Schwann cell receptor for fibrin. Experimental Cell Research, 291(2), 514–524. 10.1016/S0014-4827(03)00409-9 [PubMed: 14644171]

Curnis F, Cattaneo A, Longhi R, Sacchi A, Gasparri AM, Pastorino F, … Corti A (2010). Critical role of flanking residues in NGR-to-isoDGR transition and CD13/integrin receptor switching. Journal of Biological Chemistry, 285(12), 9114–9123. 10.1074/jbc.M109.044297

Curnis F, Longhi R, Crippa L, Cattaneo A, Dondossola E, Bachi A, & Corti A (2006). Spontaneous formation of L-isoaspartate and gain of function in fibronectin. Journal of Biological Chemistry, 281(47), 36466–36476. 10.1074/jbc.M604812200

D'Antonio M, Droggiti A, Feltri ML, Roes J, Wrabetz L, Mirsky R, & Jessen KR (2006). TGFbeta type II receptor signaling controls Schwann cell death and proliferation in developing nerves. The Journal of Neuroscience, 26(33), 8417–8427. 10.1523/JNEUROSCI.1578-06.2006 [PubMed: 16914667]

D'Antonio M, Musner N, Scapin C, Ungaro D, del Carro U, Ron D, … Wrabetz L (2013). Resetting translational homeostasis restores myelination in Charcot-Marie-Tooth disease type 1B mice. The Journal of Experimental Medicine, 210(4), 821–838. 10.1084/jem.20122005 [PubMed: 23547100]

Einheber S, Milner TA, Giancotti F, & Salzer JL (1993). Axonal regulation of Schwann cell integrin expression suggests a role for alpha 6 beta 4 in myelination. Journal of Cell Biology, 123(5), 1223–1236. 10.1083/jcb.123.5.1223

Elbaz B, Traka M, Kunjamma RB, Dukala D, Brosius Lutz A, Anton ES, … Popko B (2016). Adenomatous polyposis coli regulates radial axonal sorting and myelination in the PNS. Development, 143 (13), 2356–2366. 10.1242/dev.135913 [PubMed: 27226321]

El-Brolosy MA, Kontarakis Z, Rossi A, Kuenne C, Gunther S, Fukuda N, … Stainier DYR (2019). Genetic compensation triggered by mutant mRNA degradation. Nature, 568, 1–26. 10.1038/s41586-019-1064-z

Eshed Y, Feinberg K, Poliak S, Sabanay H, Sarig-Nadir O, Spiegel I, … Peles E (2005). Gliomedin mediates Schwann cell-axon interaction and the molecular assembly of the nodes of Ranvier. Neuron, 47(2), 215–229. 10.1016/j.neuron.2005.06.026 [PubMed: 16039564]

Feltri ML, D'Antonio M, Previtali S, Fasolini M, Messing A, & Wrabetz L (1999). P0-Cre transgenic mice for inactivation of adhesion molecules in Schwann cells. Charcot-Marie-Tooth Disorders, 883, 116–123.

Feltri ML, D-Antonio M, Quattrini A, Numerato R, Arona M, Previtali S, … Wrabetz L (1999). A novel P0 glycoprotein transgene activates expression of lacZ in myelin-forming Schwann cells. The European Journal of Neuroscience, 11(5), 1577–1586. 10.1046/j.1460-9568.1999.00568.x [PubMed: 10215910]

Feltri ML, Poitelon Y, & Previtali SC (2016). How Schwann cells Sort axons: New concepts. The Neuroscientist, 22(3), 252–265. 10.1177/1073858415572361 [PubMed: 25686621]

Feltri ML, Porta DG, Previtali SC, Nodari A, Migliavacca B, Cassetti A, … Wrabetz L (2002). Conditional disruption of $\beta 1$ integrin in Schwann cells impedes interactions with axons. Journal of Cell Biology, 156(1), 199–210. 10.1083/jcb.200109021

Feltri ML, Scherer SS, Wrabetz L, Kamholz J, & Shy ME (1992). Mitogen-expanded Schwann cells retain the capacity to myelinate regenerating axons after transplantation into rat sciatic nerve. Proceedings of the National Academy of Sciences of the United States of America, 89 (18), 8827–8831. [PubMed: 1326765]

Feltri ML, & Wrabetz L (2005). Laminins and their receptors in Schwann cells and hereditary neuropathies. Journal of the Peripheral Nervous System, 10(2), 128–143. 10.1111/j.1085-9489.2005.0010204.x [PubMed: 15958125]

Ghitti M, Spitaleri A, Valentinis B, Mari S, Asperti C, Traversari C, … Musco G (2012). Molecular dynamics reveal that isoDGR-containing cyclopeptides are true $\alpha_V\beta3$ antagonists unable to promote integrin allostery and activation. Angewandte Chemie International Edition, 51 (31), 7702–7705. 10.1002/anie.201202032 [PubMed: 22718573]

Haney CA, Sahenk Z, Li C, Lemmon VP, Roder J, & Trapp BD (1999). Heterophilic binding of L1 on unmyelinated sensory axons mediates Schwann cell adhesion and is required for axonal survival. Journal of Cell Biology, 146(5), 1173–1184.

Henderson NC, Arnold TD, Katamura Y, Giacomini MM, Rodriguez JD, McCarty JH, … Sheppard D (2013). Targeting of α_V integrin identifies a core molecular pathway that regulates fibrosis in several organs. Nature Medicine, 19(12), 1617–1624. 10.1038/nm.3282

Humphries JD (2006). Integrin ligands at a glance. Journal of Cell Science, 119(19), 3901–3903. 10.1242/jcs.03098 [PubMed: 16988024]

Hynes RO (1987). Integrins: A family of cell surface receptors. Cell, 235, 172–189. 10.1111/j.0105-2896.2010.00903.x

Hynes RO (2002a). A reevaluation of integrins as regulators of angiogenesis. Nature Medicine, 8(9), 918–921. 10.1038/nm0902-918

Hynes RO (2002b). Integrins: Bidirectional, allosteric signaling machines. Cell, 110, 673–687. [PubMed: 12297042]

Ieguchi K, Fujita M, Ma Z, Davari P, Taniguchi Y, Sekiguchi K, … Takada Y (2010). Direct binding of the EGF-like domain of neuregulin-1 to integrins ({alpha}v{beta}3 and {alpha}6{beta}4) is involved in neuregulin-1/ErbB signaling. The Journal of Biological Chemistry, 285(41), 31388–31398. 10.1074/jbc.M110.113878 [PubMed: 20682778]

Itoh K, Fushiki S, Kamiguchi H, Arnold B, Altevogt P, & Lemmon V (2005). Disrupted Schwann cell–axon interactions in peripheral nerves of mice with altered L1-integrin interactions. Molecular and Cellular Neuroscience, 30(1), 131–136. 10.1016/j.mcn.2005.06.006 [PubMed: 16039871]

Jessen KR, & Mirsky R (2005). The origin and development of glial cells in peripheral nerves. Nature Reviews. Neuroscience, 6(9), 671–682. 10.1038/nrn1746 [PubMed: 16136171]

Jin F, Dong B, Georgiou J, Jiang Q, Zhang J, Bharioke A, … Siminovitch KA (2011). N-WASp is required for Schwann cell cytoskeletal dynamics, normal myelin gene expression and peripheral nerve myelination. Development, 138(7), 1329–1337. 10.1242/dev.058677 [PubMed: 21385763]

Lacy-Hulbert A, Smith AM, Tissire H, Barry M, Crowley D, Bronson RT, … Hynes RO (2007). Ulcerative colitis and autoimmunity induced by loss of myeloid αV integrins. Proceedings of the National Academy of Sciences of the United States of America, 104(40), 15823–15828. 10.1073/pnas.0707421104 [PubMed: 17895374]

Lefcort F, Venstrom K, McDonald JA, & Reichardt LF (1992). Regulation of expression of fibronectin and its receptor, alpha 5 beta 1, during development and regeneration of peripheral nerve. Development, 116(3), 767–782. [PubMed: 1289065]

Leyton L, Schneider P, Labra CV, Rüegg C, Hetz CA, Quest AF, & Bron C (2001). Thy-1 binds to integrin beta(3) on astrocytes and triggers formation of focal contact sites. Current Biology: CB, 11(13), 1028–1038. [PubMed: 11470407]

Li C, Tropak MB, Gerlai R, Clapoff S, Abramow-Newerly W, Trapp B, … Roder J (1994). Myelination in the absence of myelin-associated glycoprotein. Nature, 369(6483), 747–750. 10.1038/369747a0 [PubMed: 7516497]

Liu WQ, Martinez JA, Durand J, Wildering W, & Zochodne DW (2009). RGD-mediated adhesive interactions are important for peripheral axon outgrowth in vivo. Neurobiology of Disease, 34(1), 11–22. 10.1016/j.nbd.2008.11.012 [PubMed: 19118630]

Ma Z, Zhu P, Shi H, Guo L, Zhang Q, Chen Y, … Chen J (2019). PTC-bearing mRNA elicits a genetic compensation response via Upf3a and COMPASS components. Nature, 568, 1–25. 10.1038/s41586-019-1057-y

McCarty JH, Lacy-Hulbert A, Charest A, Bronson RT, Crowley D, Housman D, … Hynes RO (2005). Selective ablation of alphav integrins in the central nervous system leads to cerebral hemorrhage, seizures, axonal degeneration and premature death. Development, 132(1), 165–176. 10.1242/dev.01551 [PubMed: 15576410]

McCarty JH, Monahan-Earley RA, Brown LF, Keller M, Gerhardt H, Rubin K, … Hynes RO (2002). Defective associations between blood vessels and brain parenchyma lead to cerebral hemorrhage in mice lacking α_V Integrins. Molecular and Cellular Biology, 22 (21), 7667–7677. 10.1128/mcb.22.21.7667-7677.2002 [PubMed: 12370313]

Michelson AM, Russell ES, & Harman PJ (1955). Dystrophia muscularis: A hereditary primary myopathy in the house mouse. Proceedings of the National Academy of Sciences of the United States of America, 41(12), 1079–1084. [PubMed: 16589799]

Milner R, Edwards G, Streuli C, & Ffrench-Constant C (1996). A role in migration for the αvβ1 integrin expressed on oligodendrocyte precursors. Journal of Neuroscience, 16(22), 7240–7252. 10.1523/JNEUROSCI.16-22-07240.1996 [PubMed: 8929432]

Milner R, & Ffrench-Constant C (1994). A developmental analysis of oligodendroglial integrins in primary cells: Changes in alpha v-associated beta subunits during differentiation. Development, 120(12), 3497–3506. [PubMed: 7821217]

Milner R, Frost E, Nishimura S, Delcommenne M, Streuli C, Pytela R, & Constant CF (1997). Expression of $\alpha_V\beta3$ and $\alpha_V\beta8$ integrins during oligodendrocyte precursor differentiation in the presence and absence of axons. Glia, 21(4), 350–360. 10.1002/(SICI)1098-1136(199712)21:4<350::AID-GLIA2>3.0.CO;2-7 [PubMed: 9419010]

Milner R, Wilby M, Nishimura S, Boylen K, Edwards G, Fawcett J, … Ffrench-Constant C (1997). Division of labor of Schwann cell integrins during migration on peripheral nerve extracellular matrix ligands. Developmental Biology, 185(2), 215–228. 10.1006/dbio.1997.8547 [PubMed: 9187084]

Mobley AK, Tchaicha JH, Shin J, Hossain MG, & McCarty JH (2009). β8 integrin regulates neurogenesis and neurovascular homeostasis in the adult brain. Journal of Cell Science, 122(13), 2322–2322. 10.1242/jcs.055939

Monk KR, Feltri ML, & Taveggia C (2015). New insights on Schwann cell development. Glia, 63(8), 1376–1393. 10.1002/glia.22852 [PubMed: 25921593]

Montani L, Buerki-Thurnherr T, de Faria JP, Pereira JA, Dias NG, Fernandes R, … Relvas JB (2014). Profilin 1 is required for peripheral nervous system myelination. Development, 141(7), 1553–1561. 10.1242/dev.101840 [PubMed: 24598164]

Montgomery AM, Becker JC, Siu CH, Lemmon VP, Cheresh DA, Pancook JD, … Reisfeld RA (1996). Human neural cell adhesion molecule L1 and rat homologue NILE are ligands for integrin alpha v beta 3. Journal of Cell Biology, 132(3), 475–485.

Nardone G, la Cruz JOD, Vrbsky J, Martini C, Pribyl J, Skladal P, … Forte G (2017). YAP regulates cell mechanics by controlling focal adhesion assembly. Nature Communications, 8, 1–13. 10.1038/ncomms15321

Nath D, Slocombe PM, Stephens PE, Warn A, Hutchinson GR, Yamada KM, … Murphy G (1999). Interaction of metargidin (ADAM-15) with alphavbeta3 and alpha5beta1 integrins on different haemopoietic cells. Journal of Cell Science, 112(Pt 4), 579–587. [PubMed: 9914169]

Nodari A, Zambroni D, Quattrini A, Court FA, D'Urso A, Recchia A, … Feltri ML (2007). Beta1 integrin activates Rac1 in Schwann cells to generate radial lamellae during axonal sorting and myelination. Journal of Cell Biology, 177(6), 1063–1075. 10.1083/jcb.200610014

Novak N, Bar V, Sabanay H, Frechter S, Jaegle M, Snapper SB, … Peles E (2011). N-WASP is required for membrane wrapping and myelination by Schwann cells. Journal of Cell Biology, 192(2), 243–250. 10.1083/jcb.201010013

Occhi S, Zambroni D, del Carro U, Amadio S, Sirkowski EE, Scherer SS, … Feltri ML (2005). Both laminin and Schwann cell dystroglycan are necessary for proper clustering of sodium channels at nodes of Ranvier. The Journal of Neuroscience, 25(41), 9418–9427. 10.1523/JNEUROSCI.2068-05.2005 [PubMed: 16221851]

Owens GC, Boyd CJ, Bunge RP, & Salzer JL (1990). Expression of recombinant myelin-associated glycoprotein in primary Schwann cells promotes the initial investment of axons by myelinating Schwann cells. Journal of Cell Biology, 111(3), 1171–1182.

Owens GC, & Bunge RP (1989). Evidence for an early Role for myelin-associated glycoprotein in the process of myelination. Glia, 2, 119–128. 10.1002/glia.440020208 [PubMed: 2470674]

Owens GC, & Bunge RP (1990). Schwann cells depleted of galactocerebroside express myelin-associated glycoprotein and initiate but do not continue the process of myelination. Glia, 3(2), 118–124. 10.1002/glia.440030205 [PubMed: 1692007]

Owens GC, & Bunge RP (1991). Schwann cells infected with a recombinant retrovirus expressing myelin-associated glycoprotein antisense RNA do not form myelin. Neuron, 7(4), 565–575. [PubMed: 1718333]

Ozkaynak E, Abello G, Jaegle M, van Berge L, Hamer D, Kegel L, … Meijer D (2010). Adam22 is a major neuronal receptor for Lgi4-mediated Schwann cell signaling. The Journal of Neuroscience, 30(10), 3857–3864. 10.1523/JNEUROSCI.6287-09.2010 [PubMed: 20220021]

Pellegatta M, de Arcangelis A, D'Urso A, Nodari A, Zambroni D, Ghidinelli M, … Feltri ML (2013). α6β1 and α7β1 integrins are required in Schwann cells to sort axons. The Journal of Neuroscience, 33(46), 17995–18007. 10.1523/JNEUROSCI.3179-13.2013 [PubMed: 24227711]

Phillips DR, Charo IF, & Scarborough RM (1991). GPIIb-IIIa: The responsive integrin. Cell, 65(3), 359–362. 10.1016/0092-8674(91)90451-4 [PubMed: 2018971]

Poitelon Y, Bogni S, Matafora V, Nunes GD-F, Hurley E, Ghidinelli M, … Feltri ML (2015). Spatial mapping of juxtacrine axo-glial interactions identifies novel molecules in peripheral myelination. Nature Communications, 6, 1–13. 10.1038/ncomms9303

Poitelon Y, Lopez-Anido C, Catignas K, Berti C, Palmisano M, Williamson C, … Feltri ML (2016). YAP and TAZ control peripheral myelination and the expression of laminin receptors in Schwann cells. Nature Neuroscience, 19(7), 879–887. 10.1038/nn.4316 [PubMed: 27273766]

Previtali SC, Nodari A, Taveggia C, Pardini C, Dina G, Villa A, … Feltri ML (2003). Expression of laminin receptors in Schwann cell differentiation: Evidence for distinct roles. The Journal of Neuroscience, 23(13), 5520–5530. [PubMed: 12843252]

Qian Y, Zhao X, Han Q, Chen W, Li H, & Yuan W (2018). An integrated multi-layer 3D-fabrication of PDA/ RGD coated graphene loaded PCL nanoscaffold for peripheral nerve restoration. Nature Communications, 9, 1–16. 10.1038/s41467-017-02598-7

Quattrini A, Previtali S, Feltri ML, Canal N, Nemni R, & Wrabetz L (1996). β4 integrin and other Schwann cell markers in axonal neuropathy. Glia, 17(4), 294–306. 10.1002/(SICI)1098-1136(199608)17:4<294::AID-GLIA4>3.0.CO;2-# [PubMed: 8856326]

Rafiuddin Ahmed M, & Jayakumar R (2003). Peripheral nerve regeneration in RGD peptide incorporated collagen tubes. Brain Research, 993 (1–2), 208–216. 10.1016/j.brainres.2003.08.057 [PubMed: 14642848]

Reed NI, Jo H, Chen C, Tsujino K, Arnold TD, DeGrado WF, & Sheppard D (2015). The $\alpha_V\beta1$ integrin plays a critical in vivo role in tissue fibrosis. Science Translational Medicine, 7(288), 288ra79–288ra79. 10.1126/scitranslmed.aaa5094

Ruoslahti E (1996). RGD and other recognition sequences for integrins. Annual Review of Cell and Developmental Biology, 12(1), 697–715. 10.1146/annurev.cellbio.12.1.697

Salzer JL (2015). Schwann cell myelination. Cold Spring Harbor Perspectives in Biology, 7(8), a020529–a020527. 10.1101/cshperspect.a020529 [PubMed: 26054742]

Schwartz MA, & Ginsberg MH (2002). Networks and crosstalk: Integrin signalling spreads. Nature Cell Biology, 4(4), E65–E68. 10.1038/ncb0402-e65 [PubMed: 11944032]

Seals DF, & Courtneidge SA (2003). The ADAMs family of metalloproteases: Multidomain proteins with multiple functions. Genes & Development, 17(1), 7–30. 10.1101/gad.1039703 [PubMed: 12514095]

Shaw CE, Milner R, Compston AS, & Ffrench-Constant C (1996). Analysis of integrin expression on oligodendrocytes during axo-glial interaction by using rat-mouse xenocultures. Journal of Neuroscience, 16(3), 1163–1172. [PubMed: 8558245]

Spitaleri A, Mari S, Curnis F, Traversari C, Longhi R, Bordignon C, … Musco G (2008). Structural basis for the interaction of isoDGR with the RGD-binding site of alphavbeta3 integrin. Journal of Biological Chemistry, 283(28), 19757–19768. 10.1074/jbc.M710273200

Taveggia C, Zanazzi G, Petrylak A, Yano H, Rosenbluth J, Einheber S, … Salzer JL (2005). Neuregulin-1 type III determines the ensheathment fate of axons. Neuron, 47(5), 681–694. 10.1016/j.neuron.2005.08.017 [PubMed: 16129398]

Teräväinen TP, Myllymäki SM, Friedrichs J, Strohmeyer N, Moyano JV, Wu C, … Manninen A (2013). αV-Integrins are required for mechanotransduction in MDCK epithelial cells. PLoS One, 8(8), e71485–e71415. 10.1371/journal.pone.0071485 [PubMed: 23977051]

Turner CJ, Badu-Nkansah K, Crowley D, van der Flier A, & Hynes RO (2015). α5 and α_V integrins cooperate to regulate vascular smooth muscle and neural crest functions in vivo. Development, 142(4), 797–808. 10.1242/dev.117572 [PubMed: 25670798]

van der Flier A, Badu-Nkansah K, Whittaker CA, Crowley D, Bronson RT, Lacy-Hulbert A, & Hynes RO (2010). Endothelial alpha5 and alphav integrins cooperate in remodeling of the vasculature during development. Development, 137(14), 2439–2449. 10.1242/dev.049551 [PubMed: 20570943]

Yamazaki S, Ema H, Karlsson G, Yamaguchi T, Miyoshi H, Shioda S, … Nakauchi H (2011). Nonmyelinating Schwann cells maintain hematopoietic stem cell hibernation in the bone marrow niche. Cell, 147(5), 1146–1158. 10.1016/j.cell.2011.09.053 [PubMed: 22118468]

Yang JT, Bader BL, Kreidberg JA, Ullman-Culleré M, Trevithick JE, & Hynes RO (1999). Overlapping and independent functions of fibronectin receptor integrins in early mesodermal development. Developmental Biology, 215(2), 264–277. 10.1006/dbio.1999.9451 [PubMed: 10545236]

Yang JT, & Hynes RO (1996). Fibronectin receptor functions in embryonic cells deficient in alpha 5 beta 1 integrin can be replaced by alpha V integrins. Molecular Biology of the Cell, 7(11), 1737–1748. [PubMed: 8930896]

Yu WM (2005). Schwann cell-specific ablation of Laminin 1 causes apoptosis and prevents proliferation. Journal of Neuroscience, 25(18), 4463–4472. 10.1523/JNEUROSCI.5032-04.2005 [PubMed: 15872093]

Yu WM, Chen ZL, North AJ, & Strickland S (2009). Laminin is required for Schwann cell morphogenesis. Journal of Cell Science, 122 (7), 929–936. 10.1242/jcs.033928 [PubMed: 19295124]

Zheng J, Kontoveros D, Lin F, Hua G, Reneker DH, Becker ML, & Willits RK (2015). Enhanced Schwann cell attachment and alignment using one-pot “dual click” GRGDS and YIGSR derivatized nanofibers. Biomacromolecules, 16(1), 357–363. 10.1021/bm501552t [PubMed: 25479181]

Zhou M, Graham R, Russell G, & Croucher PI (2001). MDC-9 (ADAM-9/Meltrin γ) functions as an adhesion molecule by binding the αVβ5 integrin. Biochemical and Biophysical Research Communications, 280(2), 574–580. 10.1006/bbrc.2000.4155 [PubMed: 11162558]

Zimmerman L, Lendahl U, Cunninghum M, McKay R, Parr B, Gavin B, … McMahon A (1994). Independent regulatory elements in the nestin gene direct transgene expression to neural stem-cells or muscle precursors. Neuron, 12(1), 11–24. [PubMed: 8292356]

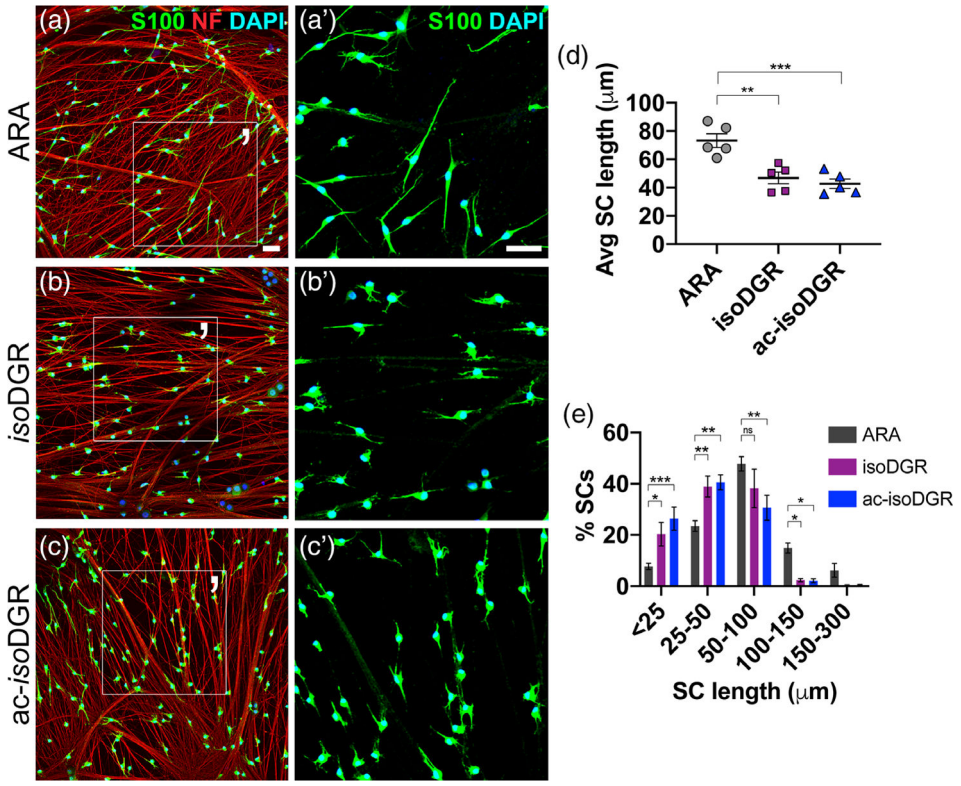

FIGURE 1.

Antagonist peptides that block RGD-binding integrins delay process extension of Schwann cells plated on axons. (a–c) WT cultured SCs pretreated with either (a) ARA (negative control), (b) *iso*DGR, or (c) ac-*iso*DGR antagonists. Peptides were seeded on untreated WT DRG neurons for 3.5 hr, then fixed and costained with anti-S100 Ab (green, labels SCs), anti-neurofilament (NF) Ab (red, labels neurons), and nuclear DAPI (blue). (a′–c′) Magnified area of (a–c). Scale bar is 50 μm in all panels. (d) Average (Avg) SC length in each cohort (student's *t* test; *ARA*: $n = 5$ replicates, 1,880 total cells quantified; isoDGR: $n = 5$ replicates, 2,305 total cells quantified; ac-isoDGR: $n = 5$ replicates, 2,122 total cells quantified; *SEM* error bars). Compared to ARA, the average SC length decreased in *iso*DGR (−36%) and ac-*iso*DGR (−41%) cohorts. (e) SC lengths categorized into bins. In *iso*DGR and ac-*iso*DGR cohorts, significantly more SCs were stunted (<25 μm), more had short processes (25–50 μm), and fewer lengthened (50–100 μm) compared to ARA cohort (ordinary two-way analysis of variance (ANOVA), $n = 5$ replicates, *SEM* error bars). DRG, dorsal root ganglia; SC, Schwann cell

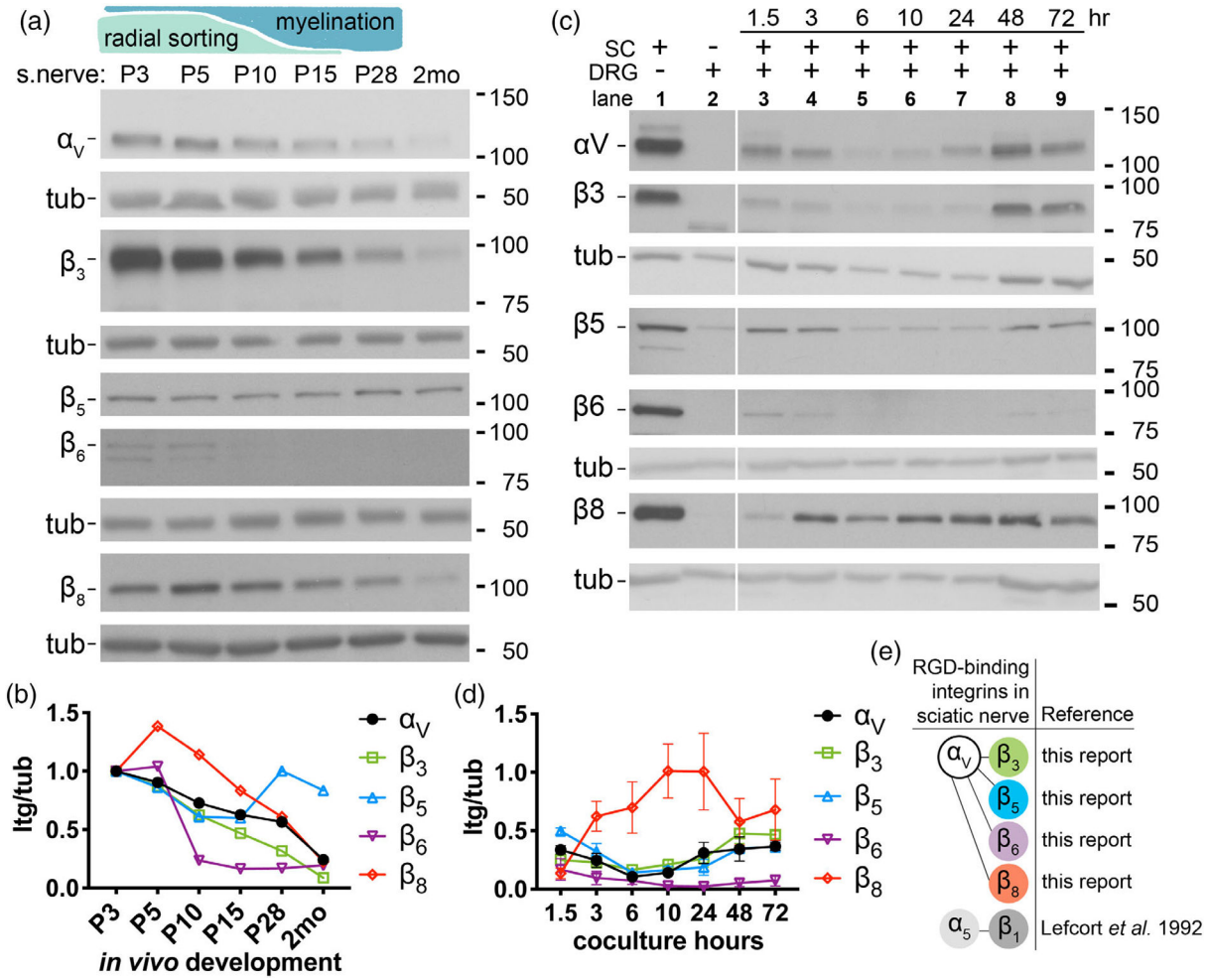

FIGURE 2.

Integrin subunit α_V and its known β partners are expressed in sciatic nerves during early postnatal development. (a) Schematic: Radial sorting in mice begins around birth, is most active at P3–P5, and concludes around P10–P15. Myelination follows radial sorting and completes around P28. Immunoblot of sciatic nerves (s.nerve) from P3 to 2-month old WT mice probed with anti-integrin α_V, $-\beta_3$, $-\beta_5$, $-\beta_6$, and $-\beta_8$ Abs. β-tubulin (tub) was used as loading control. (b) Expression of each subunit as ratio of integrin/tubulin. Levels were normalized to P3 from the same immunoblot. See Supporting Information Figure S2 for full blots. (c) Immunoblot of cultured WT SCs (Lane 1), DRGs (Lane 2), and SCs + DRGs cocultured for 1.5, 3, 6, 10, 24, 48, and 72 hr (Lanes 3–9). Immunoblot is representative of three biological experiments. Error bars indicate *SEM*; $n = 3$. (d) Expression of each subunit as ratio of integrin/tubulin. Levels were normalized to Lane 1 from the same immunoblot. (e) RGD-binding integrins expressed in sciatic nerve, with references. SC, Schwann cell

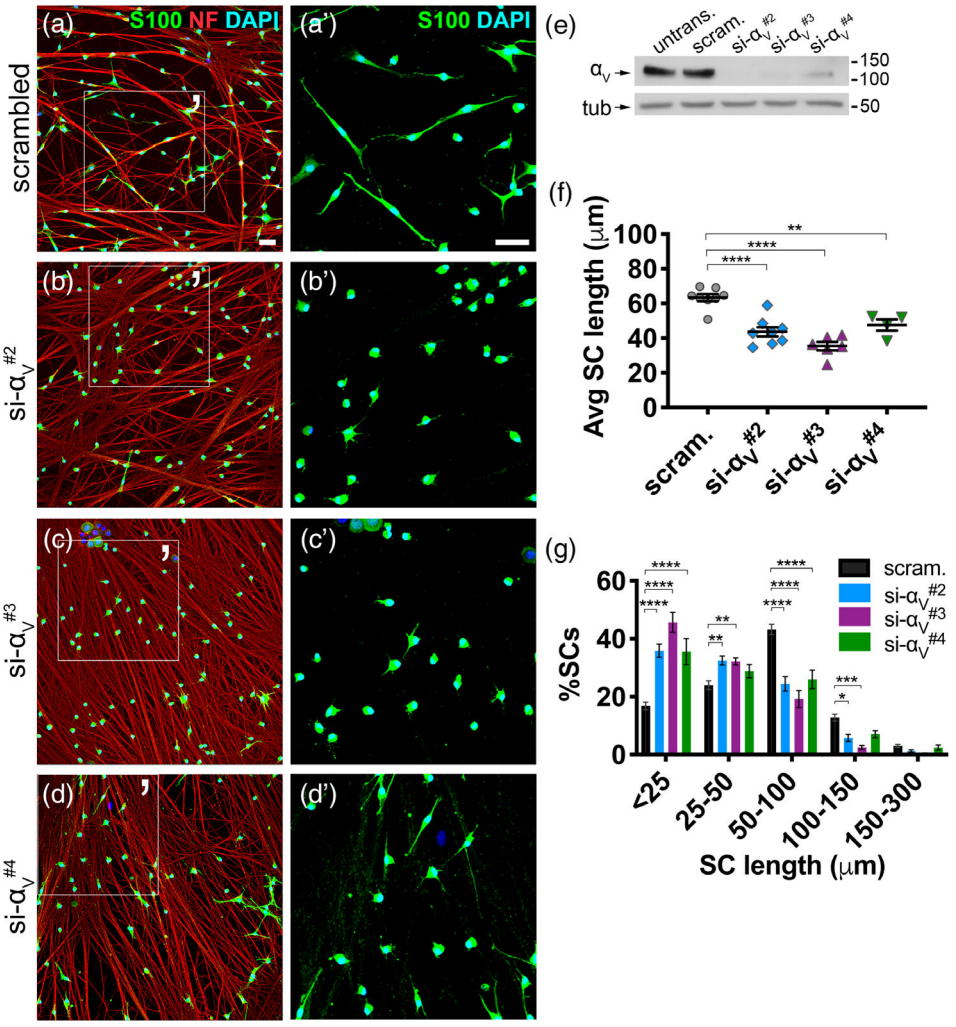

FIGURE 3.

Silencing the integrin subunit α_V in SCs phenocopies the effect of RGD antagonists in SCs. (a–d) SCs were transfected with scrambled siRNA (scram., negative control) or one of three sequences targeting the integrin α_V subunit (si-$\alpha_V^{\#2}$, -$\alpha_V^{\#3}$, -$\alpha_V^{\#4}$), then cocultured with untreated WT DRG neurons for 3.5 hr. Cultures were stained with S100 (green), neurofilament (NF) (red), and DAPI (blue) to label SCs, neurons, and nuclei, respectively. (a′–d′) Magnified area of (a–d). Scale bar is 50 μm in all panels. (e) Immunoblot of untransfected (untrans.), scrambled (scram), and si-α_V-treated SCs to confirm α_V protein knockdown. (f) Average (Avg) SC length in each cohort (student's t test; scrambled: $n = 8$ replicates, 3,365 total cells quantified; si-$\alpha_V^{\#2}$: $n = 8$ replicates, 3,563 total cells quantified; si-$\alpha_V^{\#3}$: $n = 6$ replicates, 2,548 total cells quantified; si-$\alpha_V^{\#4}$: $n = 4$ replicates, 1,451 total cells quantified; *SEM* error bars). Compared to negative control, average length decreased in si-$\alpha_V^{\#2}$ (−31%), si-$\alpha_V^{\#3}$ (−44%), and si-$\alpha_V^{\#4}$ (−25%) cohorts. (g) SC lengths categorized into bins. Significantly more α_V-silenced SCs were stunted (<25 μm), more had short processes (25–50 μm), and fewer lengthened (50–100 μm and 100–150 μm) compared to negative control (ordinary two-way analysis of variance (ANOVA), $n = \geq 4$ coverslips, *SEM* error bars)

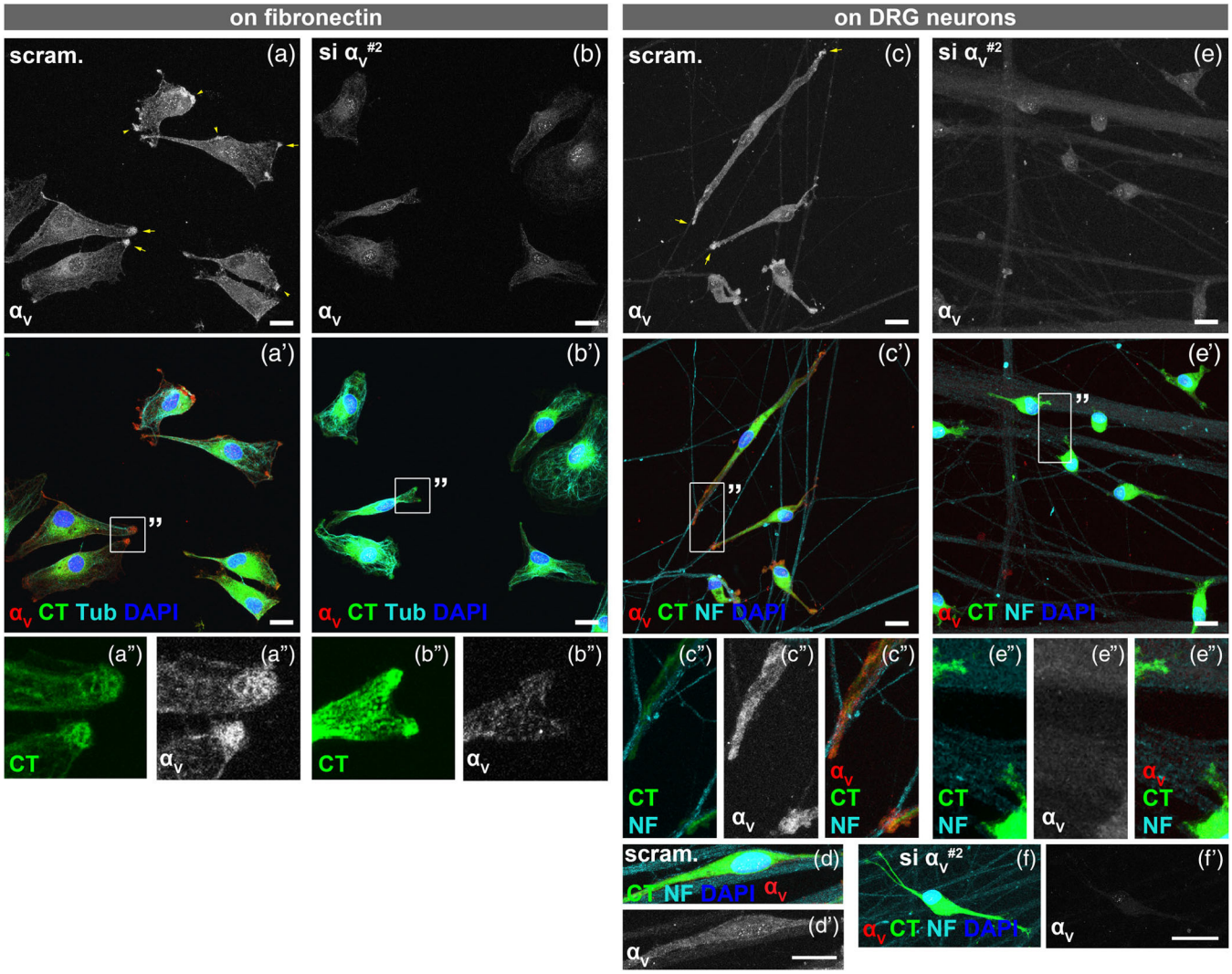

FIGURE 4.

α_V integrins are enriched at tips of Schwann cell (SC) protrusions. (a,b) Scrambled- and si-$\alpha_V^{\#2}$-treated SCs were labeled with cell tracker (CT) green, then plated on fibronectin (FN)-coated coverslips for 3.5 hr. Cells were costained with anti-α_V Ab (red), anti-tubulin Ab (Tub, cyan), and DAPI (blue). (a/a′/a′′) α_V integrin was detected at tips of protruding lamellae, particularly at membrane ruffles (arrowheads) and leading edges (arrows). (b/b′/b′′) α_V-silenced SCs lacked α_V integrin immunoreactivity at the tips. Also, the diffused cytoplasmic staining diminished. (c/c′/c′′) When seeded on neurons for 3.5 hr, α_V integrin concentrated at tips of the SC process and at sites of axon contact (arrows). Cells were costained with anti-neurofilament (NF) Ab (cyan) to label neurons. (d/d′) In contrast, α_V integrin was absent along the body of already elongated SCs on axons. (e/e′/e′′,f/f′) α_V-silenced SCs with short (e/e′/e′′) or long (f) processes had no α_V integrin immunoreactivity. All are Z-stack images acquired using identical confocal settings. Scale bar = 30 μm in all panels. Images are representative of at least four replicates. SCs were seeded on neurons at a density of 20,000

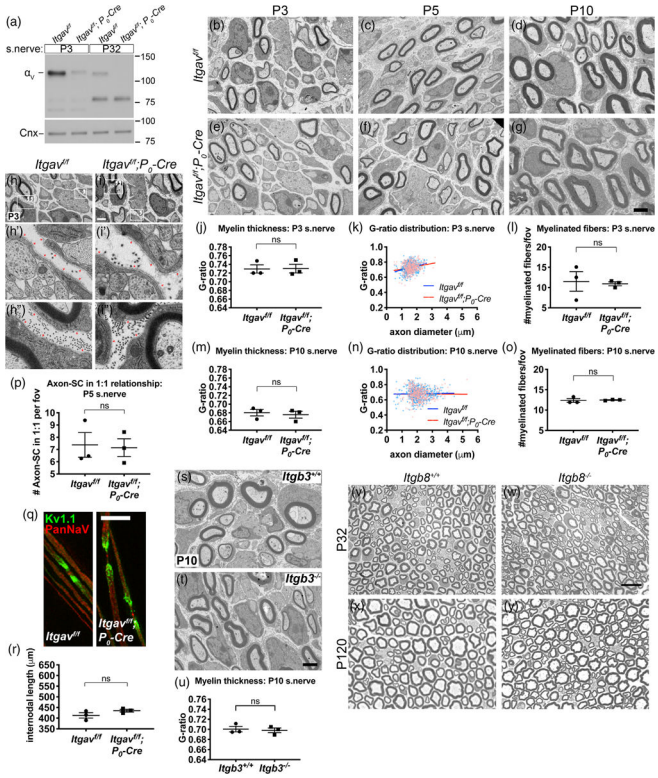

FIGURE 5.

Myelination in vivo proceeds normally in the absence of all α_V-containing integrins in Schwann cells (SCs). (a) The integrin subunit α_V was deleted specifically in SCs using P_0-Cre and *Itgav*-floxed (*Itgav*$^{f/f}$) mice. Immunoblot of sciatic nerves shows that α_V protein decreased in *Itgav*$^{f/f}$; *P*$_0$-*Cre* (cKO) compared to controls (*Itgav*$^{f/f}$) at P3 (−84% by densitometry analysis) and P32 (−96% by densitometry analysis). Bands below 100 kDa are likely nonspecific. (b–g) No obvious defects in electron micrograph (EM) cross sections of P3, P5, and P10 cKO sciatic nerves. Scale bar for (b–g) is 2 μm. (h–i) Basal lamina was continuous and appeared to form normally around axon bundles (h′,i′, red arrows) and individually myelinated fibers (h′′,i′′, red arrows) in cKO sciatic nerves at P3. Scale bar for (h,i) is 2 μm. (j–p) Quantification of several myelination parameters indicates normal myelination in cKO. Average G-ratio (≥120 fibers quantified per animal) (j,m), G-ratio distribution (k,n), and average number of myelinated fibers per field of view (fov, a 282 μm^2 area, ≥13 fields quantified per animal) (l,o) were comparable between control and cKO at P3 and P10 (student's *t* test; *n* = 3 animals/genotype). Error bars represent *SEM*. (p) Average number of axon/SC units engaged in 1:1 relationship was not statistically different between *Itgav*$^{f/f}$ and *Itgav*$^{f/f}$; *P*$_0$-*Cre* at P5 (student's *t* test, *n* = 3 animals/genotype, ≥18 fields [282 μm^2 area] quantified per animal, *SEM* error bars). (q) To assess nodal organization, teased adult nerve fibers were immunostained for nodal marker PanNaV (red) to label Na^+ channels and juxtaparanodal marker Kv1.1 (green) to label K^+ channels. No defects were evident in cKO nerve fibers. Scale bar is 25 μm. (r) Average internodal length did not statistically differ between control and cKO nerves (student's *t* test, *n* = 3 animals/genotype, ≥106 internodes quantified per genotype, *SEM* error bars). (s,t) Electron micrograph (EM) cross sections of P10 sciatic nerves from *Itgb3*$^{+/+}$ and *Itgb3*$^{-/-}$ mice show no myelination defects. Scale bar

is 2 μm. (u) Average G-ratios in *Itgb3*$^{+/+}$ and *Itgb3*$^{-/-}$ at P10 are comparable (student's *t* test, $n = 3$ animals/genotype, ≥50 fibers quantified per animal, *SEM* error bars). β_3 integrin protein absence was confirmed in Supporting Information Figure S4c. (v–y) Semithin cross sections of sciatic nerves from *Itgb8*$^{+/+}$ and *Itgb8*$^{-/-}$ mice at P32 (v–w) and P120 (x,y) show no obvious morphological defects in integrin β_8 mutants. Scale bar for (v–y) is 12.5 μm

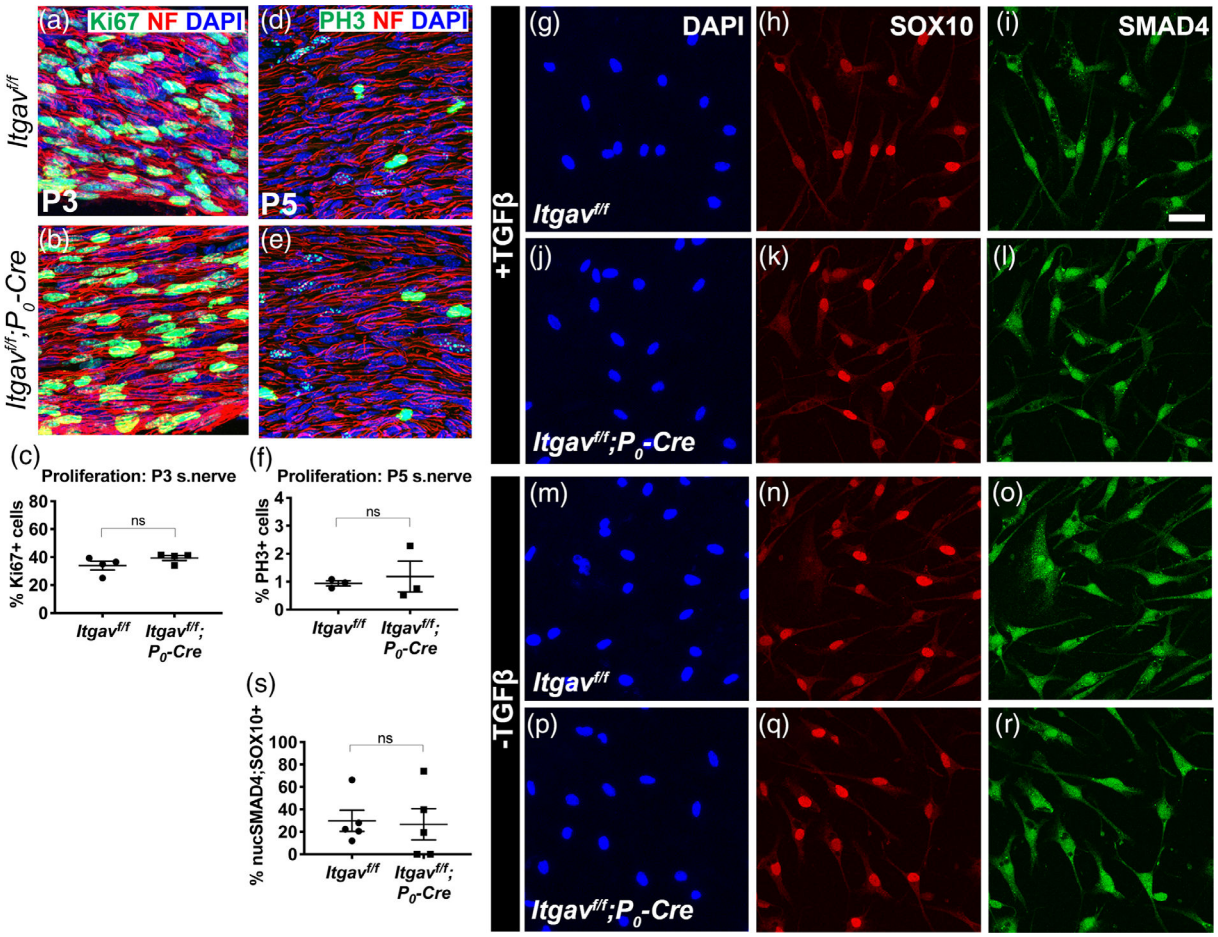

FIGURE 6.

Schwann cells (SCs) lacking integrin α_V proliferate and respond to TFGβ1 normally. (a,b,d,e) Longitudinal sections of *Itgav*$^{f/f}$ and *Itgav*$^{f/f}$; *P*$_0$-*Cre* sciatic nerves were immunostained for proliferation markers Ki67 (green) at P3 (a,b) and PH3 (green) at P5 (d,e). Both were costained with neurofilament (NF) (red) and DAPI (blue). (c,f) No appreciable difference in the percentage of Ki67-positive cells (student's *t* test, $n = 4$ nerves) or of PH3-positive cells (student's *t* test, $n = 3$ animals/genotype, *SEM* error bars) was detected between *Itgav*$^{f/f}$ and *Itgav*$^{f/f}$; *P*$_0$-*Cre*. (g–r) SMAD4 was properly shuttled to the nucleus in α_V mutant cells. SCs isolated from *Itgav*$^{f/f}$ or *Itgav*$^{f/f}$; *P*$_0$-*Cre* sciatic nerves were cultured, treated with TGFβ1, then immunostained for SOX10 (to identify SCs), SMAD4, and DAPI. SMAD4 localized more in the cytoplasm of untreated cells (m–r), but when treated with TFGβ1, SMAD4 localized more in the nucleus of both *Itgav*$^{f/f}$ and *Itgav*$^{f/f}$; *P*$_0$-*Cre* SCs (g–l). Scale bar for (g-r) is 30 μm. (s) Average %nuclear-SMAD4/Sox10-positive cells were comparable between *Itgav*$^{f/f}$ and *Itgav*$^{f/f}$; *P*$_0$-*Cre* (student's *t* test, $n = 5$ animals/genotype, ≥1,370 Sox10-positive cells quantified per genotype, *SEM* error bars). Mean %Sox10-positive cells: *Itgav*$^{f/f}$ 51%, *Itgav*$^{f/f}$; *P*$_0$-*Cre* 67%

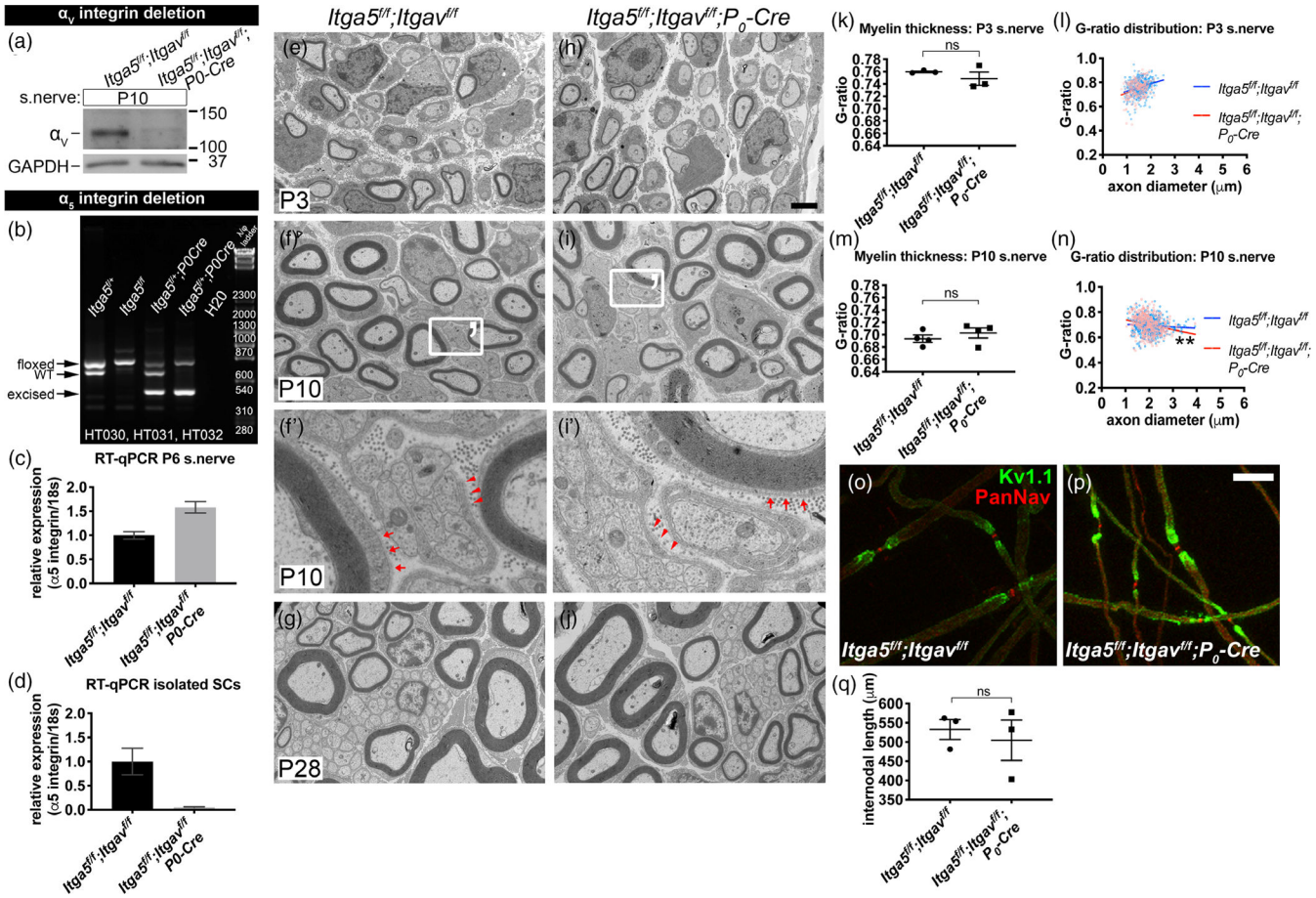

FIGURE 7.

Myelination in vivo proceeds in the absence of α_5 and α_V integrins in SCs. (a-d) Assessment of α_5 and α_V expression in *Itga5*$^{f/f}$; *Itgav*$^{f/f}$ (control) and *Itga5*$^{f/f}$; *Itgav*$^{f/f}$; *P*$_0$-*Cre* (conditional double knockout [cdKO]). (a) Immunoblot confirmed that α_V integrin protein decreased in P10 cdKO sciatic nerves compared to control. GAPDH was used as loading control. (b) Multiplex PCR (using HT030, −31, −32 primers) of genomic DNA from sciatic nerves showed that the *Itga5*-floxed gene was excised in cdKO nerves. See Supporting Information Figure S5a–c for details. (c) Real-time quantitative PCR (RT-qPCR) of P6 nerves showed that α_5 integrin mRNA increased in cdKO (+58%) compared to control. Results are from one experiment with three independent replicates: control ΔCt 19.3 ± 0.06 *SD*, cdKO ΔCt 18.6 ± 0.06 *SD*. (d) RT-qPCR of cultured SCs isolated from control and cdKO nerves showed that α_5 mRNA levels were markedly decreased in cdKO SC (−95%). Results are from one experiment with three independent replicates: control ΔCt 7.6 ± 0.4 *SD*, cdKO ΔCt 11.9 ± 0.3 *SD*. Relative expression for (c) and (d) shown as $2^{-(\Delta\Delta Ct)}$ value with *SD* errors bars. (e–j) Electron micrograph (EM) cross sections of P3 (e,h), P10 (f,i), and P28 (g,j) sciatic nerves from control and cdKO mice showed no obvious difference. Scale bar for (e–i, g–j) is 2 μm. (f′,i′) Magnified region of (f,i) shows that myelinated fibers (arrows) and axon bundles (arrowheads) at P10 in control and cdKO are surrounded by a continuous basal lamina. (k,m) Average G-ratios at P3 and P10 were similar between control and cdKO (student's *t* test, *n* = ≥3 animals/genotype, ≥50 fibers quantified per animal,

SEM error bars). (l,n) G-ratio distribution for P3 and P10. Difference in G-ratio distribution between control and cdKO at P10 was statistically significant (linear regression analysis of slopes, $^{**}p = .003$ for P10, ns for P3). (o,p) Teased adult nerve fibers stained for PanNaV (red) and Kv1.1 (green) showed normal nodal organization in cdKO. Scale bar is 25 μm. (q) Average internodal length was similar between control and cdKO (student's *t* test, $n = 3$ animals/genotype, ≥102 internodes quantified per genotype, *SEM* error bars)

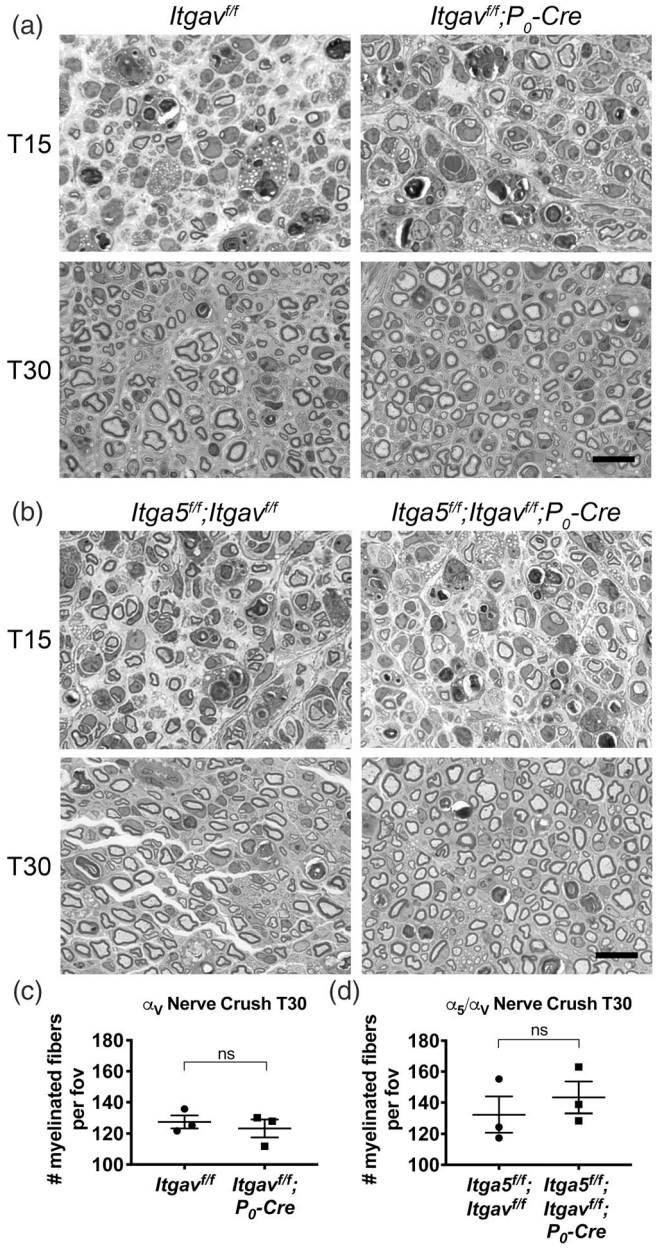

FIGURE 8.

Schwann cells (SCs) lacking integrins α_5 and α_V in vivo can remyelinate and regenerate the nerve after injury. (a) Adult *Itgav*$^{f/f}$ and *Itgav*$^{f/f}$; P_0-*Cre* sciatic nerves were crushed, then examined at 15 (T15) and 30 (T30) days postcrush. Shown are semithin cross sections of portion of nerve distal to the crush site. Remyelination and axon regeneration in α_V cKO appeared similar to controls. Scale bars are 12.5 μm. (b) Nerve crush was repeated in *Itga5*$^{f/f}$; *Itgav*$^{f/f}$ and *Itga5*$^{f/f}$; *Itgav*$^{f/f}$; P_0-*Cre* adults. No morphological difference was detected between controls and α_5/α_V conditional double knockout (cdKO). Scale bars are 12.5 μm. (c,d) Average number of myelinated fibers per 140 cm^2 area (field of view [fov])

in α_V(c) and α_5/α_V (d) at T30. Differences were not statistically significant in both cohorts (student's *t* test, $n = 3$ animals/genotype, ≥5 fields quantified per animal)